

1 Event History Analysis for psychological time-to-event data: A tutorial in R with examples
2 in Bayesian and frequentist workflows

3 Sven Panis¹ & Richard Ramsey¹

4 ¹ ETH Zürich

5 Author Note

6 Neural Control of Movement lab, Department of Health Sciences and Technology
7 (D-HEST). Social Brain Sciences lab, Department of Humanities, Social and Political
8 Sciences (D-GESS).

9 The authors made the following contributions. Sven Panis: Conceptualization,
10 Writing - Original Draft Preparation, Writing - Review & Editing; Richard Ramsey:
11 Conceptualization, Writing - Review & Editing, Supervision.

12 Correspondence concerning this article should be addressed to Sven Panis, ETH
13 GLC, room G16.2, Gloriustrasse 37/39, 8006 Zürich. E-mail: sven.panis@hest.ethz.ch

14

Abstract

15 Time-to-event data such as response times, saccade latencies, and fixation durations form a
16 cornerstone of experimental psychology, and have had a widespread impact on our
17 understanding of human cognition. However, the orthodox method for analysing such data
18 – comparing means between conditions – is known to conceal valuable information about
19 the timeline of psychological effects, such as their onset time and duration. The ability to
20 reveal finer-grained, “temporal states” of cognitive processes can have important
21 consequences for theory development by qualitatively changing the key inferences that are
22 drawn from psychological data. Luckily, well-established analytical approaches, such as
23 event history analysis (EHA), are able to evaluate the detailed shape of time-to-event
24 distributions, and thus characterise the time course of psychological states. One barrier to
25 wider use of EHA, however, is that the analytical workflow is typically more
26 time-consuming and complex than orthodox approaches. To help achieve broader uptake,
27 in this paper we outline a set of tutorials that detail how to implement one distributional
28 method known as discrete-time EHA. We illustrate how to wrangle raw data files and
29 calculate descriptive statistics, as well as how to calculate inferential statistics via Bayesian
30 and frequentist multilevel regression modelling. Along the way, we touch upon several key
31 aspects of the workflow, such as how to specify regression models, the implications for
32 experimental design, as well as how to manage inter-individual differences. We finish the
33 article by considering the benefits of the approach for understanding psychological states,
34 as well as the limitations and future directions of this work. Finally, the project is written
35 in R and freely available, which means the general approach can easily be adapted to other
36 data sets, and all of the tutorials are available as .html files to widen access beyond R-users.

37 *Keywords:* response times, event history analysis, Bayesian multi-level regression
38 models, experimental psychology, cognitive psychology

39 Word count: X

40

1. Introduction

41 1.1 Motivation and background context: Comparing means versus 42 distributional shapes

43 In experimental psychology, it is standard practice to analyse response times (RTs),
44 saccade latencies, and fixation durations by calculating average performance across a series
45 of trials. Such mean-average comparisons have been the workhorse of experimental
46 psychology over the last century, and have had a substantial impact on theory development
47 as well as our understanding of the structure of cognition and brain function. However,
48 differences in mean RT conceal important pieces of information, such as when an
49 experimental effect starts, how long it lasts, how it evolves with increasing waiting time,
50 and whether its onset is time-locked to other events (Panis, 2020; Panis, Moran,
51 Wolkersdorfer, & Schmidt, 2020; Panis & Schmidt, 2016, 2022; Panis, Torfs, Gillebert,
52 Wagemans, & Humphreys, 2017; Panis & Wagemans, 2009; Wolkersdorfer, Panis, &
53 Schmidt, 2020). Such information is useful not only for the interpretation of experimental
54 effects under investigation, but also for cognitive psychophysiology and computational
55 model selection (Panis, Schmidt, Wolkersdorfer, & Schmidt, 2020).

56 As a simple illustration, Figure 1 shows the results of several simulated RT data sets,
57 which show how mean-average comparisons between two conditions can conceal the shape
58 of the underlying RT distributions. For instance, in examples 1-3, mean RT is always
59 comparable between two conditions, while the distributions differ (Figure 1, left). In
60 contrast, in examples 4-6, mean RT is lower in condition 2 compared to condition 1, but
61 the RT distributions differ in each case (Figure 1, right). Therefore, a comparison of means
62 would lead to a similar conclusion in examples 1-3, as well as examples 4-6, whereas a
63 comparison of the distributions would lead to a different conclusion in every case.

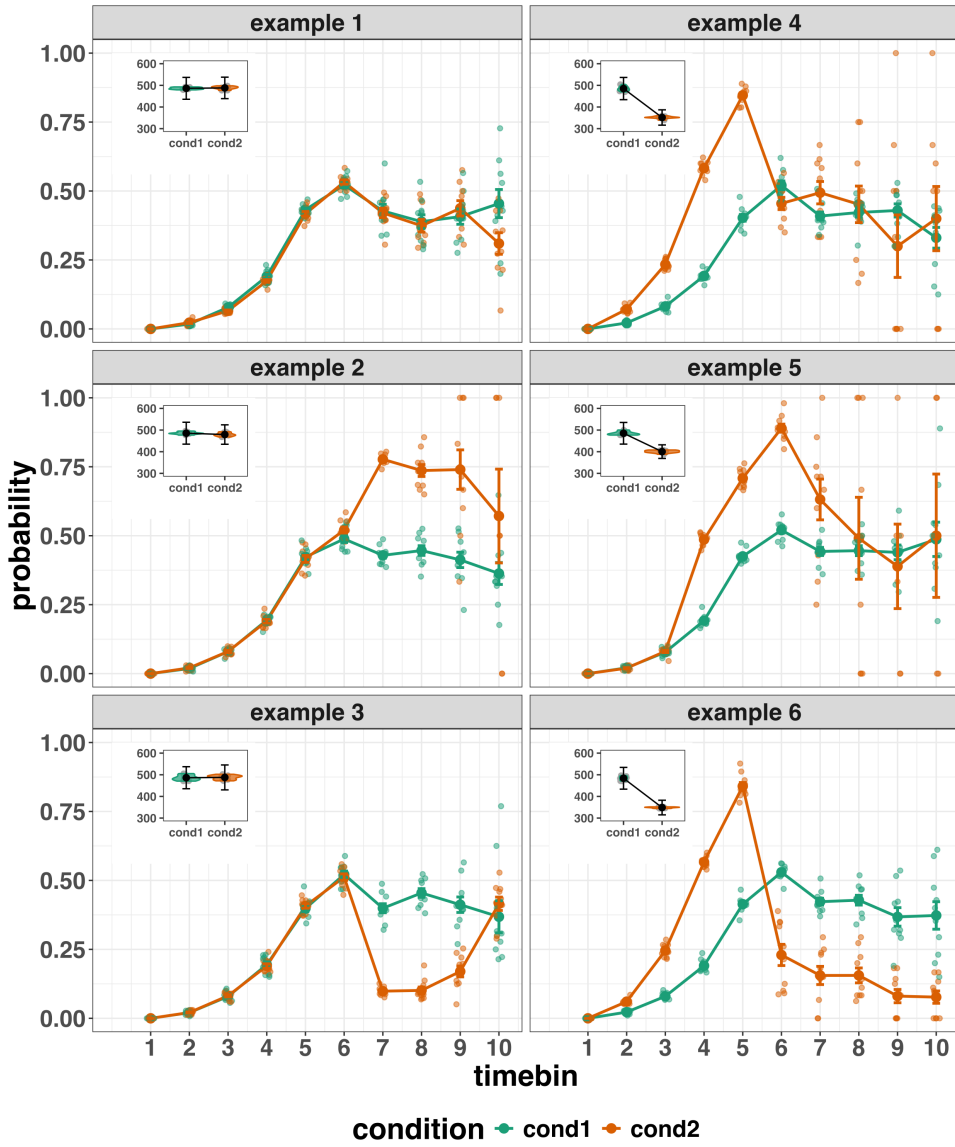


Figure 1. Means versus distributional shapes for six different simulated data set examples.

The first second after stimulus onset is divided in ten bins of 100 ms. Timebin indicates the bin rank. The first bin is (0,100], the last bin is (900,1000]. For our purposes here, it is enough to know that the distributions plotted represent the probability of an event occurring in that timebin, given that it has not yet occurred. Insets show mean response time per condition.

65 data across trials, a distributional approach offers the possibility to reveal the time course
66 of psychological states. As such, the approach permits different kinds of questions to be
67 asked, different inferences to be made, and it holds the potential to discriminate between
68 different theoretical accounts of psychological and/or brain-based processes. For example,
69 the distributions in Example 4 show that the effect starts between 100 and 200 ms (in
70 timebin 2) and is gone when the waiting time reaches 500 ms or more. In contrast, in
71 Example 5, the effect starts around 300 ms and is gone by 700 ms. And in the Example 6,
72 the effect reverses between 500 and 600 ms. What kind of theory or theories could account
73 for such effects? Are there new auxiliary assumptions that theories need to adopt? And are
74 there new experiments that need to be performed to test the novel predictions that follow
75 from these analyses? As we show later using published examples, for many psychological
76 questions, such “temporal states” information can be theoretically meaningful by leading to
77 more fine-grained understanding of psychological processes, as well as adding a relatively
78 under-used dimension – the passage of time – to the theory building toolkit.

79 From a historical perspective, it is worth noting that the development of analytical
80 tools that can estimate or predict whether and when events will occur is not a new
81 endeavour. Indeed, hundreds of years ago, analytical methods were developed to predict
82 the duration of time until people died (e.g., Halley, 1997; Makeham, William M., 1860).
83 The same logic has been applied to psychological time-to-event data, as previously
84 demonstrated (Panis, Schmidt, et al., 2020).

85 1.2 Aims and structure of the paper

86 In this paper, we focus on a distributional method for time-to-event data known as
87 discrete-time Event History Analysis (EHA), a.k.a. survival analysis, hazard analysis,
88 duration analysis, failure-time analysis, and transition analysis (Singer & Willett, 2003).
89 We hope to show the value of EHA for knowledge and theory building in cognitive
90 psychology and related areas of research, such as cognitive neuroscience. Most importantly,

91 we provide tutorials that provide step-by-step code and instructions in the hope that we
92 can enable others to use EHA in a more routine, efficient and effective manner.

93 We first provide a brief overview of EHA to orient the reader to the basic concepts
94 that we will use throughout the paper. However, this will remain relatively short, as this
95 has been covered in detail before (Allison, 1982, 2010; Singer & Willett, 2003). Indeed, our
96 primary aim here is to introduce the set of tutorials, which explain **how** to do such
97 analyses, rather than repeat in any detail **why** you may do them.

98 We provide six different tutorials, which are written in the R programming language
99 and publicly available on our Github and the Open Science Framework (OSF) pages, along
100 with all of the other code and material associated with the project. The tutorials provide
101 hands-on, concrete examples of key parts of the analytical process, so that others can apply
102 EHA to their own time-to-event data sets. Each tutorial is provided as an RMarkdown file,
103 so that others can download and adapt the code to fit their own purposes. Additionally,
104 each tutorial is made available as a .html file, so that it can be viewed by any web browser,
105 and thus available to those that do not use R. Finally, the manuscript itself is written in R
106 using the papaja package (Aust & Barth, 2024), which makes it computationally
107 reproducible, in terms of the underlying data and figures.

108 In Tutorial 1a, we illustrate how to process or “wrangle” a previously published RT +
109 accuracy data set to calculate descriptive statistics when there is one independent variable.
110 The descriptive statistics are plotted, and we comment on their interpretation. In Tutorial
111 1b we provide a generalisation of this approach to illustrate how one can calculate the
112 descriptive statistics when using a more complex design, such as when there are two
113 independent variables.

114 In Tutorial 2a, we illustrate how one can fit Bayesian multi-level regression models to
115 RT data using the R package brms. We also perform prior predictive checks, compare
116 models, and interpret the plots of the predicted hazard functions for the selected model,

117 and the posterior distributions of our contrasts of interest. In Tutorial 2b we fit Bayesian
118 multi-level regression models to *timed* accuracy data to perform a micro-level
119 speed-accuracy tradeoff (SAT) analysis, which complements the EHA of RT data for choice
120 RT data.

121 In Tutorial 3a, we shortly illustrate how to fit similar multilevel regression models for
122 RT data in a frequentist framework using the R package lme4. We then briefly compare
123 and contrast these inferential frameworks when applied to EHA. In Tutorial 3b, we
124 illustrate how to perform the SAT analysis in a frequentist framework.

125 In tutorial 4, we illustrate one approach to planning how much data to collect in an
126 experiment using EHA. We use data simulation techniques to vary sample size and trial
127 count per condition until a certain degree of statistical power or precision is reached.
128 [[more to come here, once we have written the tutorial]].

129 In summary, even though EHA is a widely used statistical tool and there already exist
130 many excellent reviews (e.g., Blossfeld & Rohwer, 2002; Box-Steffensmeier, 2004; Hosmer,
131 Lemeshow, & May, 2011; Teachman, 1983) and tutorials (e.g., Allison, 2010; Landes,
132 Engelhardt, & Pelletier, 2020) on its general use-cases, we are not aware of any tutorials
133 that are aimed at psychological time-to-event data, and which provide worked examples of
134 the key data processing and multi-level regression modelling steps. Therefore, our ultimate
135 goal is twofold: first, we want to convince readers of the many benefits of using EHA when
136 dealing with time-to-event data with a focus on psychological time-to-event data, and
137 second, we want to provide a set of practical tutorials, which provide step-by-step
138 instructions on how you actually perform a discrete-time EHA on time-to-event data such
139 as RT data, as well as a complementary discrete-time SAT analysis on timed accuracy data.

2. A brief introduction to event history analysis

For a comprehensive background context to EHA, we recommend several excellent textbooks (Allison, 2010; Singer & Willett, 2003). Likewise, for a general introduction to understanding regression equations, we recommend several excellent textbooks (Gelman, Hill, & Vehtari, 2020; Winter, 2019). Our focus here is not on providing a detailed account of the underlying regression equations, since this topic has been comprehensively covered many times before. Instead, we want to provide an intuition regarding how EHA works in general, as well as in the context of experimental psychology. As such, we only supply regression equations in part D of the supplementary material.

2.1 Basic features of event history analysis

To apply EHA, one must be able to:

1. define an event of interest that represents a qualitative change that can be situated in time (e.g., a button press, a saccade onset, a fixation offset, etc.);
2. define time point zero (e.g., target stimulus onset, fixation onset, etc.);
3. measure the passage of time between time point zero and event occurrence in discrete or continuous time units.

In EHA, the definition of hazard and the type of models employed depend on whether one is using continuous or discrete time units. Since our focus here is on hazard models that use discrete time units, we describe that approach. After dividing time in discrete, contiguous time bins indexed by t (e.g., $t = 1:10$ timebins), let RT be a discrete random variable denoting the rank of the time bin in which a particular person's response occurs in a particular experimental condition. For example, the first response might occur at 546 ms and it would be in timebin 6 (any RTs from 501 ms to 600 ms).

163 Discrete-time EHA focuses on the discrete-time hazard function of event occurrence

164 and the discrete-time survivor function (Figure 2). The equations that define both of these

165 functions are reported in part A of the supplementary material. The discrete-time hazard

166 function gives you, for each time bin, the probability that the event occurs (sometime) in

167 bin t , given that the event does not occur in previous bins. In other words, it reflects the

168 instantaneous likelihood that the event occurs in the current bin, given that it has not yet

169 occurred in the past, i.e., in one of the prior bins. In contrast, the discrete-time survivor

170 function cumulates the bin-by-bin risks of event *nonoccurrence* to obtain the survival

171 probability, the probability that the event occurs after bin t . In other words, the survivor

172 function gives you for each time bin the likelihood that the event occurs in the future, i.e.,

173 in one of the subsequent timebins.

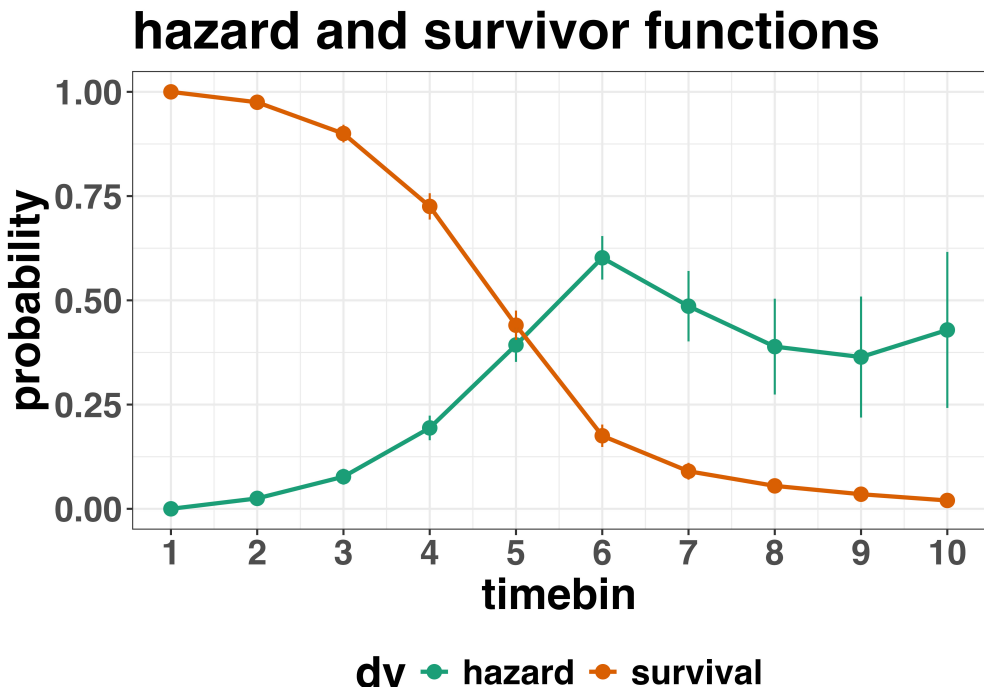


Figure 2. Discrete-time hazard and survivor functions. Discrete time-to-event data were simulated for 200 trials of 1 experimental condition. While the hazard function is the vehicle for inferring the time course of cognitive processes, the survival probability $S(t-1)$ can help to qualify or provide context to the interpretation of the hazard probability $h(t)$. For example, the high hazard of $.60 = h(t=6)$ is experienced only by 44 percent of the trials, as $S(t=5) = .44$. Because the survivor function is a decreasing function of time, the error bars in later parts of the hazard function will always be wider and less precise compared to earlier parts.

¹⁷⁴ **2.2 Benefits of event history analysis**

¹⁷⁵ Statisticians and mathematical psychologists recommend focusing on the hazard
¹⁷⁶ function when analyzing time-to-event data for various reasons. We do not cover these
¹⁷⁷ benefits in detail here, as these are more general topics that have been covered elsewhere in
¹⁷⁸ textbooks. Instead, we briefly summarise list the benefits below, and refer the reader to
¹⁷⁹ section F of Supplementary Materials for more detailed coverage of the benefits. A
¹⁸⁰ summary of the benefits are as follows:

- 181 1. Hazard functions are more diagnostic than density functions when one is interested in
182 studying the detailed shape of a RT distribution (Holden et al., 2009).
- 183 2. RT distributions may differ from each other in multiple ways, and hazard functions
184 allow one to capture these differences which mean-average comparisons may conceal
185 (Townsend, 1990).
- 186 3. EHA takes account of more of the data collected in a typical speeded response
187 experiment, by virtue of not discarding right-censored observations. Trials with very
188 long RTs are not discarded, but instead contribute to the risk set in each time bin
189 (see below).
- 190 4. Hazard modeling allows one to incorporate time-varying explanatory covariates, such
191 as heart rate, electroencephalogram (EEG) signal amplitude, gaze location, etc.
192 (Allison, 2010). This is useful for linking physiological effects to behavioral effects
193 when performing cognitive psychophysiology (Meyer, Osman, Irwin, & Yantis, 1988).
- 194 5. EHA can help to solve the problem of model mimicry, i.e., the fact that different
195 computational models can often predict the same mean RTs as observed in the
196 empirical data, but not necessarily the detailed shapes of the empirical RT hazard
197 distributions. As such, EHA can be a tool to help distinguish between competing
198 theories of cognition and brain function.

199 2.3 Event history analysis in the context of experimental psychology

200 To make EHA more relevant to researchers studying cognitive psychology and

201 cognitive neuroscience, in this section we provide a relevant worked example and consider
202 implications that are relevant to that domain of research.

203 **2.3.1 A worked example.** In the context of experimental psychology, it is

204 common for participants to be presented with either a 1-button detection task or a

discrimination task. For example, a task may involve choosing between two response options with only one of them being correct. For such two-choice RT data, the discrete-time EHA of the RT data (hazard and survivor functions) can be extended with a discrete-time SAT analysis of the timed accuracy data. Specifically, the hazard function of event occurrence can be extended with the discrete-time conditional accuracy function, which gives you the probability that a response is correct given that it is emitted in time bin t (Allison, 2010; Kantowitz & Pachella, 2021; Wickelgren, 1977). We refer to this extended (hazard + conditional accuracy) analysis for choice RT data as EHA/SAT.

Integrating results between hazard and conditional accuracy functions for choice RT data can be informative for understanding psychological processes. To illustrate, we consider a hypothetical choice RT example that is inspired by real data (Panis & Schmidt, 2016), but simplified to make the main point clearer (Figure 3). In a standard priming paradigm, there is a prime stimulus (e.g., an arrow pointing left or right) followed by a target stimulus (another arrow pointing left or right). The prime can then be congruent or incongruent with the target.

Figure 3 shows that the early upswing in hazard is equal for both priming conditions, and that early emitted responses are always correct in the congruent condition and always incorrect in the incongruent condition. These results show that for short waiting times (< bin 6), responses always follow the prime (and not the target, as instructed). During timebin 6 the target-triggered response channel is activated and causes response competition – $ca(6) = .5$ – and a lower hazard probability in the incongruent condition. For waiting times of 600 ms or more, the hazard of response occurrence is lower in incongruent compared to congruent trials, and all responses emitted in these late bins are correct.

This joint pattern of results is interesting because it can provide meaningfully different conclusions about psychological processes compared to conventional analyses, such as computing mean-average RT and accuracy across trials. Mean-average RT would only

²³¹ represent the overall ability of cognition to overcome interference, on average, across trials.
²³² For instance, if mean-average RT was higher in incongruent than congruent trials, one may
²³³ conclude that cognitive mechanisms that support interference control are working as
²³⁴ expected across trials, and are indexed by each recorded response. But such a conclusion is
²³⁵ not supported when the effects are explored over a timeline. Instead, the psychological
²³⁶ conclusion is much more nuanced and suggests that multiple states start, stop and possibly
²³⁷ interact over a particular temporal window.

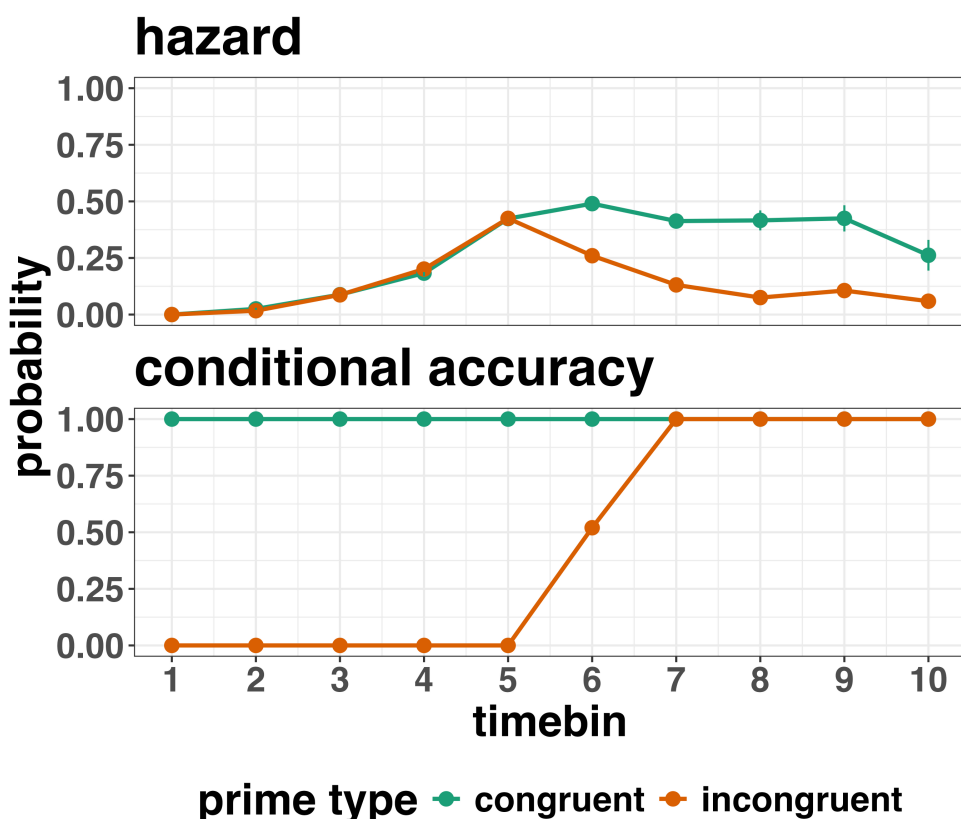


Figure 3. Discrete-time hazard and conditional accuracy functions. Discrete time-to-event and conditional accuracy data were simulated for 2000 trials for each of two priming conditions (congruent and incongruent prime stimuli). Bin width equals 100 ms.

²³⁸ Unlocking the temporal states of cognitive processes can be revealing for theory
²³⁹ development and the understanding of basic psychological processes. Possibly more

240 importantly, however, is that it simultaneously opens the door to address many new and
241 previously unanswered questions. Do all participants show similar temporal states or are
242 there individual differences? Do such individual differences extend to those individuals that
243 have been diagnosed with some form of psychopathology? How do temporal states relate to
244 brain-based mechanisms that might be studied using other methods from cognitive
245 neuroscience? And how much of theory in cognitive psychology would be in need of
246 revision if mean-average comparisons were supplemented with a temporal states approach?

247 **2.3.2 Implications for designing experiments.** Performing EHA in
248 experimental psychology has implications for how experiments are designed. Indeed, if
249 trials are categorised as a function of when responses occur, then each timebin will only
250 include a subset of the total number of trials. For example, let's consider an experiment
251 where each participant performs 2 conditions and there are 100 trial repetitions per
252 condition. Those 100 trials must be distributed in some manner across the chosen number
253 of bins.

254 In such experimental designs, since the number of trials per condition are spread
255 across bins, it is important to have a relatively large number of trial repetitions per
256 participant and per condition. Accordingly, experimental designs using this approach
257 typically focus on factorial, within-subject designs, in which a large number of observations
258 are made on a relatively small number of participants (so-called small- N designs). This
259 approach emphasizes the precision and reproducibility of data patterns at the individual
260 participant level to increase the inferential validity of the design (Baker et al., 2021; Smith
261 & Little, 2018).

262 In contrast to the large- N design that typically average across many participants
263 without being able to scrutinize individual data patterns, small- N designs retain crucial
264 information about the data patterns of individual observers. This can be advantageous
265 whenever participants differ systematically in their strategies or in the time courses of their
266 effects, so that averaging them would lead to misleading data patterns. Note that because

267 statistical power derives both from the number of participants and from the number of
268 repeated measures per participant and condition, small- N designs can still achieve what
269 are generally considered acceptable levels of statistical power, if they have a sufficient
270 amount of data overall (Baker et al., 2021; Smith & Little, 2018).

271 **3. An overview of the general analytical workflow**

272 Although the focus is on EHA/SAT, we also want to briefly comment on broader
273 aspects of our general analytical workflow, which relate more to data science and data
274 analysis workflows.

275 **3.1 Data science workflow and descriptive statistics**

276 We perform data wrangling following tidyverse principles and a functional
277 programming approach (Wickham, Çetinkaya-Rundel, & Grolemund, 2023). Functional
278 programming basically means you don't write your own loops but instead use functions
279 that have been built and tested by others. [[more here, as necessary]].

280 **3.2 Inferential statistical approach**

281 Our lab adopts a estimation approach to multi-level regression (Kruschke & Liddell,
282 2018; Winter, 2019), which is heavily influenced by the Bayesian framework as suggested
283 by Richard McElreath (Kurz, 2023b; McElreath, 2018). We also use a “keep it maximal”
284 approach to specifying varying (or random) effects (Barr, Levy, Scheepers, & Tily, 2013).
285 This means that wherever possible we include varying intercepts and slopes per participant
286 To make inferences, we use two main approaches. We compare models of different
287 complexity, using information criteria (e.g., WAIC) and cross-validation (e.g., LOO), to
288 evaluate out-of-sample predictive accuracy (McElreath, 2018). We also take the most
289 complex model and evaluate key parameters of interest using point and interval estimates.

²⁹⁰ **3.3 Implementation**

²⁹¹ We used R (Version 4.4.0; R Core Team, 2024)¹ for all reported analyses. The
²⁹² content of the tutorials, in terms of EHA and multi-level regression modelling, is mainly
²⁹³ based on Allison (2010), Singer and Willett (2003), McElreath (2018), Heiss (2021), Kurz
²⁹⁴ (2023a), and Kurz (2023b).

²⁹⁵ **4. Tutorials**

²⁹⁶ Tutorials 1a and 1b show how to calculate and plot the descriptive statistics of
²⁹⁷ EHA/SAT when there are one and two independent variables, respectively. Tutorials 2a
²⁹⁸ and 2b illustrate how to use Bayesian multilevel modeling to fit hazard and conditional
²⁹⁹ accuracy models, respectively. Tutorials 3a and 3b show how to implement, respectively,
³⁰⁰ multilevel models for hazard and conditional accuracy in the frequentist framework.
³⁰¹ Additionally, to further simplify the process for other users, the first two tutorials rely on a
³⁰² set of our own custom functions that make sub-processes easier to automate, such as data
³⁰³ wrangling and plotting functions (see part B in the supplemental material for a list of the

¹ We, furthermore, used the R-packages *bayesplot* (Version 1.11.1; Gabry, Simpson, Vehtari, Betancourt, & Gelman, 2019), *brms* (Version 2.21.0; Bürkner, 2017, 2018, 2021), *citr* (Version 0.3.2; Aust, 2019), *cmdstanr* (Version 0.8.1.9000; Gabry, Češnovar, Johnson, & Broder, 2024), *dplyr* (Version 1.1.4; Wickham, François, Henry, Müller, & Vaughan, 2023), *forcats* (Version 1.0.0; Wickham, 2023a), *ggplot2* (Version 3.5.1; Wickham, 2016), *lme4* (Version 1.1.35.5; Bates, Mächler, Bolker, & Walker, 2015), *lubridate* (Version 1.9.3; Grolemund & Wickham, 2011), *Matrix* (Version 1.7.0; Bates, Maechler, & Jagan, 2024), *nlme* (Version 3.1.166; Pinheiro & Bates, 2000), *papaja* (Version 0.1.2.9000; Aust & Barth, 2023), *patchwork* (Version 1.2.0; Pedersen, 2024), *purrr* (Version 1.0.2; Wickham & Henry, 2023), *RColorBrewer* (Version 1.1.3; Neuwirth, 2022), *Rcpp* (Eddelbuettel & Balamuta, 2018; Version 1.0.12; Eddelbuettel & François, 2011), *readr* (Version 2.1.5; Wickham, Hester, & Bryan, 2024), *RJ-2021-048* (Bengtsson, 2021), *standist* (Version 0.0.0.9000; Girard, 2024), *stringr* (Version 1.5.1; Wickham, 2023b), *tibble* (Version 3.2.1; Müller & Wickham, 2023), *tidybayes* (Version 3.0.6; Kay, 2023), *tidyverse* (Version 2.0.0; Wickham et al., 2019), and *tinylabels* (Version 0.2.4; Barth, 2023).

304 custom functions).

305 Our list of tutorials is as follows:

- 306 • 1a. Wrangle raw data and calculate descriptive stats for one independent variable
- 307 • 1b. Wrangle raw data and calculate descriptive stats for two independent variables
- 308 • 2a. Bayesian multilevel modeling for $h(t)$
- 309 • 2b. Bayesian multilevel modeling for $ca(t)$
- 310 • 3a. Frequentist multilevel modeling for $h(t)$
- 311 • 3b. Frequentist multilevel modeling for $ca(t)$
- 312 • 4. Simulation and power analysis for planning experiments

313 **4.1 Tutorial 1a: Calculating descriptive statistics using a life table**

314 **4.1.1 Data wrangling aims.** Our data wrangling procedures serve two related
315 purposes. First, we want to summarise and visualise descriptive statistics that relate to our
316 main research questions about the time course of psychological processes, using a life table.
317 A life table includes for each time bin, the risk set (i.e., the number of trials that are
318 event-free at the start of the bin), the number of observed events, and the estimates of
319 $h(t)$, $S(t)$, $P(t)$, possibly $ca(t)$, and their estimated standard errors (se).

320 Second, we want to produce two different data sets that can each be submitted to
321 different types of inferential modelling approaches. The two types of data structure we
322 label as ‘person-trial’ data and ‘person-trial-bin’ data. The ‘person-trial’ data (Table 1)
323 will be familiar to most researchers who record behavioural responses from participants, as
324 it represents the measured RT and accuracy per trial within an experiment. This data set
325 is used when fitting conditional accuracy models (Tutorials 2b and 3b).

Table 1

Data structure for ‘person-trial’ data

pid	trial	condition	rt	accuracy
1	1	congruent	373.49	1
1	2	incongruent	431.31	1
1	3	congruent	455.43	0
1	4	incongruent	622.41	1
1	5	incongruent	535.98	1
1	6	incongruent	540.08	1
1	7	congruent	511.07	1
1	8	incongruent	444.42	1
1	9	congruent	678.69	1
1	10	congruent	549.79	1

Note. The first 10 trials for participant 1 are shown. These data are simulated and for illustrative purposes only.

326 In contrast, the ‘person-trial-bin’ data (Table 2) has a different, more extended
 327 structure, which indicates in which bin a response occurred, if at all, in each trial.
 328 Therefore, the ‘person-trial-bin’ data set generates a 0 in each bin until an event occurs
 329 and then it generates a 1 to signal an event has occurred in that bin. This data set is used
 330 when fitting hazard models (Tutorials 2a and 3a). It is worth pointing out that there is no
 331 requirement for an event to occur at all (in any bin), as maybe there was no response on
 332 that trial or the event occurred after the time window of interest. Likewise, when the event
 333 occurs in bin 1 there would only be one row of data for that trial in the person-trial-bin
 334 data set.

Table 2
Data structure for ‘person-trial-bin’ data

pid	trial	condition	timebin	event
1	1	congruent	1	0
1	1	congruent	2	0
1	1	congruent	3	0
1	1	congruent	4	1
1	2	incongruent	1	0
1	2	incongruent	2	0
1	2	incongruent	3	0
1	2	incongruent	4	0
1	2	incongruent	5	1

Note. The first 2 trials for participant 1 from Table 1 are shown. The width of the time bins is 100 ms. These data are simulated and for illustrative purposes only.

335 **4.1.2 A real data wrangling example.** To illustrate how to quickly set up life
 336 tables for calculating the descriptive statistics (functions of discrete time), we use a
 337 published data set on masked response priming from Panis and Schmidt (2016). In their
 338 first experiment, Panis and Schmidt (2016) presented a double arrow for 94 ms that
 339 pointed left or right as the target stimulus with an onset at time point zero in each trial.
 340 Participants had to indicate the direction in which the double arrow pointed using their
 341 corresponding index finger, within 800 ms after target onset. Response time and accuracy
 342 were recorded on each trial. Prime type (blank, congruent, incongruent) and mask type
 343 were manipulated. Here we focus on the subset of trials in which no mask was presented.

344 The 13-ms prime stimulus was a double arrow presented 187 ms before target onset in the
 345 congruent (same direction as target) and incongruent (opposite direction as target) prime
 346 conditions.

347 There are several data wrangling steps to be taken. First, we need to load the data
 348 before we (a) supply required column names, and (b) specify the factor condition with the
 349 correct levels and labels.

350 The required column names are as follows:

- 351 • “pid”, indicating unique participant IDs;
- 352 • “trial”, indicating each unique trial per participant;
- 353 • “condition”, a factor indicating the levels of the independent variable (1, 2, ...) and
 354 the corresponding labels;
- 355 • “rt”, indicating the response times in ms;
- 356 • “acc”, indicating the accuracies (1/0).

357 In the code of Tutorial 1a, this is accomplished as follows.

```
data_wr<-read_csv("../Tutorial_1_descriptive_stats/data/DataExp1_6subjects_wrangled.csv")
colnames(data_wr) <- c("pid","bl","tr","condition","resp","acc","rt","trial")
data_wr <- data_wr %>%
  mutate(condition = condition + 1, # original levels were 0, 1, 2.
        condition = factor(condition,
                             levels=c(1,2,3),
                             labels=c("blank","congruent","incongruent")))
```

358 Next, we can set up the life tables and plots of the discrete-time functions $h(t)$, $S(t)$,
 359 $ca(t)$, and $P(t)$ – see part A of the supplementary material for their definitions. To do so
 360 using a functional programming approach, one has to nest the data within participants
 361 using the `group_nest()` function, and supply a user-defined censoring time and bin width
 362 to our custom function “`censor()`”, as follows.

```

data_nested <- data_wr %>% group_nest(pid)

data_final <- data_nested %>%
  # ! user input: censoring time, and bin width
  mutate(censored = map(data, censor, 600, 40)) %>%
  # create person-trial-bin data set
  mutate(ptb_data = map(censored, ptb)) %>%
  # create life tables without ca(t)
  mutate(lifetable = map(ptb_data, setup_lt)) %>%
  # calculate ca(t)
  mutate(condacc = map(censored, calc_ca)) %>%
  # create life tables with ca(t)
  mutate(lifetable_ca = map2(lifetable, condacc, join_lt_ca)) %>%
  # create plots
  mutate(plot = map2(.x = lifetable_ca, .y = pid, plot_eha,1))

```

363 Note that the censoring time should be a multiple of the bin width (both in ms). The

364 censoring time should be a time point after which no informative responses are expected

365 anymore. In experiments that implement a response deadline in each trial the censoring

366 time can equal that deadline time point. Trials with a RT larger than the censoring time,

367 or trials in which no response is emitted during the data collection period, are treated as

368 right-censored observations in EHA. In other words, these trials are not discarded, because

369 they contain the information that the event did not occur before the censoring time.

370 Removing such trials before calculating the mean event time will result in underestimation

371 of the true mean.

372 The person-trial-bin oriented data set is created by our custom function ptb(), and it

373 has one row for each time bin (of each trial) that is at risk for event occurrence. The

374 variable “event” in the person-trial-bin oriented data set indicates whether a response

375 occurs (1) or not (0) for each bin.

376 The next step is to set up the life table using our custom function setup_lt(),

377 calculate the conditional accuracies using our custom function `calc_ca()`, add the `ca(t)`
378 estimates to the life table using our custom function `join_lt_ca()`, and then plot the
379 descriptive statistics using our custom function `plot_eha()`. When creating the plots, some
380 warning messages will likely be generated, like these:

- 381 • Removed 2 rows containing missing values or values outside the scale range
382 (`geom_line()`).
383 • Removed 2 rows containing missing values or values outside the scale range
384 (`geom_point()`).
385 • Removed 2 rows containing missing values or values outside the scale range
386 (`geom_segment()`).

387 The warning messages are generated because some bins have no hazard and `ca(t)`
388 estimates, and no error bars. They can thus safely be ignored. One can now inspect
389 different aspects, including the life table for a particular condition of a particular subject,
390 and a plot of the different functions for a particular participant. In general, it is important
391 to visually inspect the functions first for each participant, in order to identify individuals
392 that may be guessing (e.g., a flat conditional accuracy function at .5 indicates that
393 someone is just guessing), outlying individuals, and/or different groups with qualitatively
394 different behavior.

395 Table 3 shows the life table for condition “blank” (no prime stimulus presented) for
396 participant 6.

Table 3

The life table for the blank prime condition of participant 6.

bin	risk_set	events	hazard	se_haz	survival	se_surv	ca	se_ca
0	220	NA	NA	NA	1.00	0.00	NA	NA
40	220	0	0.00	0.00	1.00	0.00	NA	NA
80	220	0	0.00	0.00	1.00	0.00	NA	NA
120	220	0	0.00	0.00	1.00	0.00	NA	NA
160	220	0	0.00	0.00	1.00	0.00	NA	NA
200	220	0	0.00	0.00	1.00	0.00	NA	NA
240	220	0	0.00	0.00	1.00	0.00	NA	NA
280	220	7	0.03	0.01	0.97	0.01	0.29	0.17
320	213	13	0.06	0.02	0.91	0.02	0.77	0.12
360	200	26	0.13	0.02	0.79	0.03	0.92	0.05
400	174	40	0.23	0.03	0.61	0.03	1.00	0.00
440	134	48	0.36	0.04	0.39	0.03	0.98	0.02
480	86	37	0.43	0.05	0.22	0.03	1.00	0.00
520	49	32	0.65	0.07	0.08	0.02	1.00	0.00
560	17	9	0.53	0.12	0.04	0.01	1.00	0.00
600	8	4	0.50	0.18	0.02	0.01	1.00	0.00

Note. The column named “bin” indicates the endpoint of each time bin (in ms), and includes time point zero. For example the first bin is (0,40] with the starting point excluded and the endpoint included. At time point zero, no events can occur and therefore $h(t=0)$ and $ca(t=0)$ are undefined. $se =$ standard error. $ca =$ conditional accuracy. $NA =$ undefined.

Figure 4 displays the discrete-time hazard, survivor, conditional accuracy, and

398 probability mass functions for each prime condition for participant 6. By using
 399 discrete-time hazard functions of event occurrence – in combination with conditional
 400 accuracy functions for two-choice tasks – one can provide an unbiased, time-varying, and
 401 probabilistic description of the latency and accuracy of responses based on all trials of any
 402 data set.

Descriptive stats for subject 6

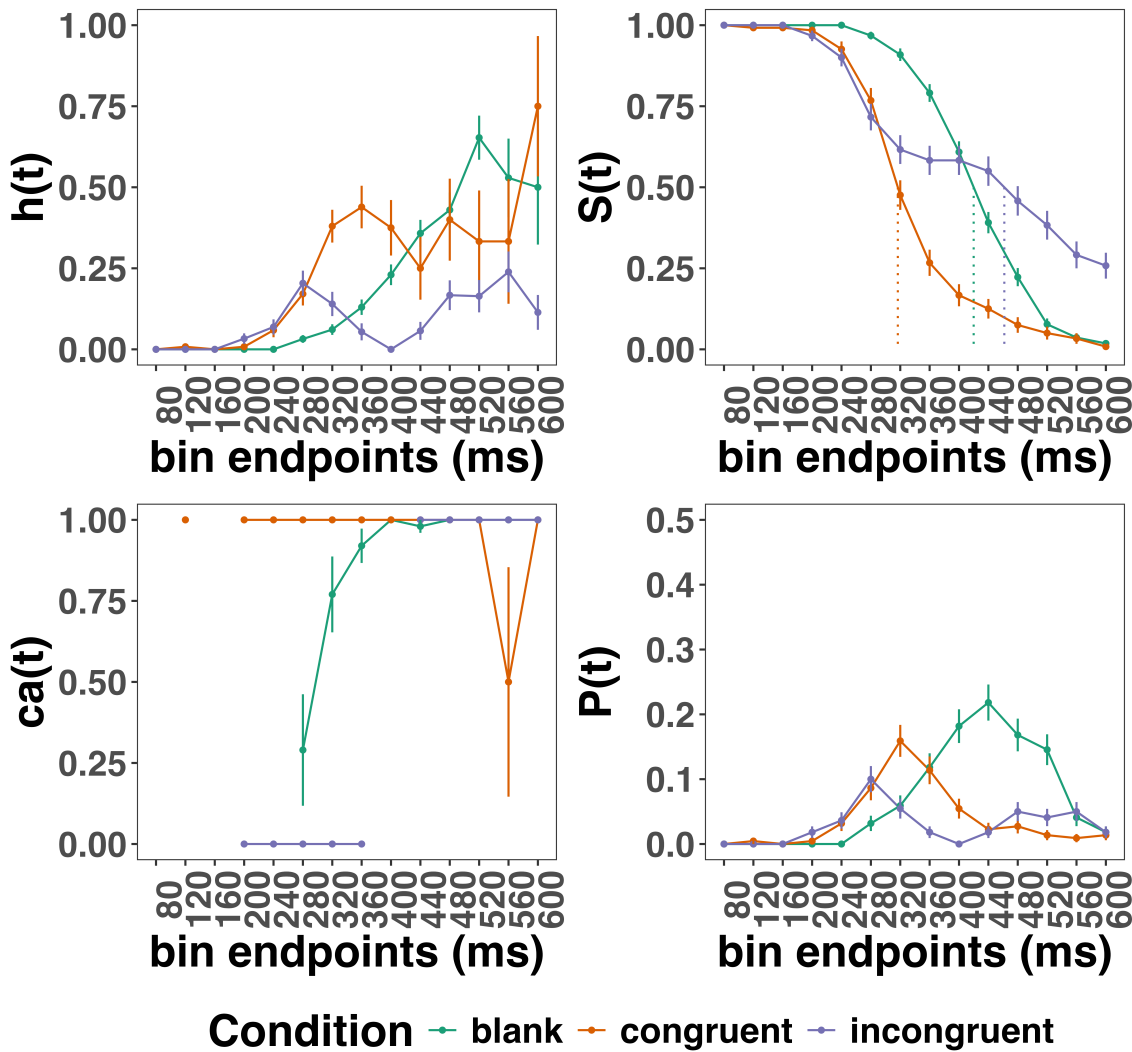


Figure 4. Estimated discrete-time hazard, survivor, probability mass, and conditional accuracy functions for participant 6. Vertical dotted lines indicate the estimated median RTs. Error bars represent +/- 1 Standard Error of the respective proportion.

403 For example, for participant 6, the estimated hazard values in bin (240,280] are 0.03,

404 0.17, and 0.20 for the blank, congruent, and incongruent prime conditions, respectively. In

405 other words, when the waiting time has increased until *240 ms* after target onset, then the

406 conditional probability of response occurrence in the next 40 ms is more than five times

407 larger for both prime-present conditions, compared to the blank prime condition.

408 Furthermore, the estimated conditional accuracy values in bin (240,280] are 0.29, 1,

409 and 0 for the blank, congruent, and incongruent prime conditions, respectively. In other

410 words, if a response is emitted in bin (240,280], then the probability that it is correct is

411 estimated to be 0.29, 1, and 0 for the blank, congruent, and incongruent prime conditions,

412 respectively.

413 However, when the waiting time has increased until *400 ms* after target onset, then

414 the conditional probability of response occurrence in the next 40 ms is estimated to be

415 0.36, 0.25, and 0.06 for the blank, congruent, and incongruent prime conditions,

416 respectively. And when a response does occur in bin (400,440], then the probability that it

417 is correct is estimated to be 0.98, 1, and 1 for the blank, congruent, and incongruent prime

418 conditions, respectively.

419 These distributional results suggest that the participant 6 is initially responding to

420 the prime even though (s)he was instructed to only respond to the target, that response

421 competition emerges in the incongruent prime condition around 300 ms, and that only

422 slower responses are fully controlled by the target stimulus. Qualitatively similar results

423 were obtained for the other five participants. When participants show qualitatively the

424 same distributional patterns, one might consider to aggregate their data and make one plot

425 (see Tutorial_1a.Rmd).

426 In general, these results go against the (often implicit) assumption in research on

427 priming that all observed responses are primed responses to the target stimulus. Instead,

428 the distributional data show that early responses are triggered exclusively by the prime

429 stimulus, while only later responses reflect primed responses to the target stimulus.

430 At this point, we have calculated, summarised and plotted descriptive statistics for
431 the key variables in EHA/SAT. As we will show in later Tutorials, statistical models for
432 $h(t)$ and $ca(t)$ can be implemented as generalized linear mixed regression models predicting
433 event occurrence (1/0) and conditional accuracy (1/0) in each bin of a selected time
434 window for analysis. But first we consider calculating the descriptive statistics for two
435 independent variables.

436 **4.2 Tutorial 1b: Generalising to a more complex design**

437 So far in this paper, we have used a simple experimental design, which involved one
438 condition with three levels. But psychological experiments are often more complex, with
439 crossed factorial designs with more conditions and more than three levels. The purpose of
440 Tutorial 1b, therefore, is to provide a generalisation of the basic approach, which extends
441 to a more complicated design. We felt that this might be useful for researchers in
442 experimental psychology that typically use crossed factorial designs.

443 To this end, Tutorial 1b illustrates how to calculate and plot the descriptive statistics
444 for the full data set of Experiment 1 of Panis and Schmidt (2016), which includes two
445 independent variables: mask type and prime type. As we use the same functional
446 programming approach as in Tutorial 1a, we simply present the sample-based functions for
447 each participant as part of Tutorial_1b.Rmd for those that are interested.

448 **4.3 Tutorial 2a: Fitting Bayesian hazard models to discrete time-to-event data**

449 In this third tutorial, we illustrate how to fit Bayesian multi-level regression models
450 to the RT data of the masked response priming data set used in Tutorial 1a. Fitting
451 (Bayesian or non-Bayesian) regression models to time-to-event data is important when you
452 want to study how the shape of the hazard function depends on various predictors (Singer

453 & Willett, 2003).

454 **4.3.1 Hazard model considerations.** There are several analytic decisions one
455 has to make when fitting a discrete-time hazard model. First, one has to select an analysis
456 time window, i.e., a contiguous set of bins for which there is enough data for each
457 participant. Second, given that the dependent variable (event occurrence) is binary, one
458 has to select a link function (see part C in the supplementary material). The cloglog link is
459 preferred over the logit link when events can occur in principle at any time point within a
460 bin, which is the case for RT data (Singer & Willett, 2003). Third, one has to choose
461 whether to treat TIME (i.e., the time bin index t) as a discrete or continuous predictor.
462 And when you treat a variable as a discrete predictor, you can choose between reference
463 coding and index coding.

464 In the case of a large- N design without repeated measurements, the parameters of a
465 discrete-time hazard model can be estimated using standard logistic regression software
466 after expanding the typical person-trial data set into a person-trial-bin data set (Allison,
467 2010). When there is clustering in the data, as in the case of a small- N design with
468 repeated measurements, the parameters of a discrete-time hazard model can be estimated
469 using population-averaged methods (e.g., Generalized Estimating Equations), and Bayesian
470 or frequentist generalized linear mixed models (Allison, 2010).

471 In general, there are three assumptions one can make or relax when adding
472 experimental predictor variables and other covariates: The linearity assumption for
473 continuous predictors (the effect of a 1 unit change is the same anywhere on the scale), the
474 additivity assumption (predictors do not interact), and the proportionality assumption
475 (predictors do not interact with TIME).

476 In tutorial_2a.Rmd we fit several Bayesian multilevel models (i.e., generalized linear
477 mixed models) that differ in complexity to the person-trial-bin oriented data set that we
478 created in Tutorial 1a. We decided to select the analysis time window (200,600] and the

479 cloglog link. Below, we shortly discuss three of these models. The person-trial-bin data set
 480 is prepared as follows.

```
# read in the file we saved in tutorial 1a
ptb_data <- read_csv("Tutorial_1_descriptive_stats/data/inputfile_hazard_modeling.csv")

ptb_data <- ptb_data %>%
  # select analysis time range: (200,600] with 10 bins (time bin ranks 6 to 15)
  filter(period > 5) %>%
  # continuous predictor for TIME named "period_9", centered on bin 9
  mutate(period_9 = period - 9,
  # categorical predictor for TIME named "timebin" with index coding
  timebin = factor(period, levels = c(6:15)),
  # factor "condition" using reference coding, with "blank" as the reference level
  condition = factor(condition, labels = c("blank", "congruent", "incongruent")),
  # categorical predictor "prime" with index coding
  prime = ifelse(condition=="blank", 1, ifelse(condition=="congruent", 2, 3)),
  prime = factor(prime, levels = c(1,2,3)))
```

481 **4.3.2 Prior distributions.** To get the posterior distribution of each model
 482 parameter given the data, we need to specify prior distributions for the model parameters
 483 which reflect our prior beliefs. In Tutorial_2a.Rmd we perform a few prior predictive
 484 checks to make sure our selected prior distributions reflect our prior beliefs (Gelman,
 485 Vehtari, et al., 2020).

486 The middle column of Figure 16 in part E of the supplementary material shows six
 487 examples of prior distributions for an intercept on the logit and/or cloglog scales. While a
 488 normal distribution with relatively large variance is often used as a weakly informative
 489 prior for continuous dependent variables, rows A and B in Figure 16 show that specifying
 490 such distributions on the logit and cloglog scales actually leads to rather informative
 491 distributions on the original probability scale, as most mass is pushed to probabilities of 0
 492 and 1.

493 **4.3.3 Model M0i: A null model with index coding.** When you do not want to

494 make assumptions about the shape of the hazard function, or its shape is not smooth but
 495 irregular, then you can use a general specification of TIME, i.e., fit one grand intercept per
 496 time bin. In this first model, we use a general specification of TIME using index coding,
 497 and do not include experimental predictors. We call this model “M0i”.

498 Before we fit model M0i, we select the necessary columns from the data, and specify

499 our priors. In the code of Tutorial 2a, model M0i is specified as follows.

```
model_M0i <-
  brm(data = data_M0i,
       family = bernoulli(link="cloglog"),
       formula = event ~ 0 + timebin + (0 + timebin | pid),
       prior = priors_M0i,
       chains = 4, cores = 4,
       iter = 3000, warmup = 1000,
       control = list(adapt_delta = 0.999,
                      step_size = 0.04,
                      max_treedepth = 12),
       seed = 12, init = "0",
       file = "Tutorial_2_Bayesian/models/model_M0i")
```

500 After selecting the bernoulli family and the cloglog link, the model formula is

501 specified. The specification “0 + . . . ” removes the default intercept in brm(). The fixed
 502 effects include an intercept for each level of timebin. Each of these intercepts is allowed to
 503 vary across individuals (variable pid). We request 2000 samples from the posterior
 504 distribution for each of four chains. Estimating model M0i took about 30 minutes on a
 505 MacBook Pro (Sonoma 14.6.1 OS, 18GB Memory, M3 Pro Chip).

506 **4.3.4 Model M1i: Adding the effects of prime-target congruency.** Previous

507 research has shown that psychological effects typically change over time (Panis, 2020;

508 Panis, Moran, et al., 2020; Panis & Schmidt, 2022; Panis et al., 2017; Panis & Wagemans,

509 2009). In the next model, therefore, we use index coding for both TIME (variable

510 “timebin”) and the categorical predictor prime-target-congruency (variable “prime”), so

511 that we get 30 grand intercepts, one for each combination of timebin level and prime level.

512 Here is the model formula of this model that we call “M1i”.

```
event ~ 0 + timebin:prime + (0 + timebin:prime | pid)
```

513 Estimating model M1i took about 124 minutes.

514 **4.3.4 Model M1d: A more parsimonious model.** When the shape of the

515 hazard function is rather smooth, as it is for behavioral RT data, one can fit a more

516 parsimonious model by treating TIME as a continuous variable, and use a polynomial

517 specification of the effect of TIME. Thus, if we want to make assumptions about (1) how

518 hazard changes over TIME in the reference condition (blank prime), and (2) how the effect

519 of congruent and incongruent primes change over TIME (relax the proportionality

520 assumption), then we can switch to a dummy coding approach for prime-target congruency

521 (variable “condition”) and treat TIME as a continuous variable (variable “period_9”).

522 For example, we may assume that hazard can change in a linear + quadratic fashion

523 over time for a blank prime, and that the effects of congruent and incongruent primes

524 relative to blank change in a linear + quadratic fashion, and fit the model called “M1d”.

525 Here is its model formula.

```
event ~ 0 + Intercept + condition*period_9 + condition*period_9_sq +
          (1 + condition*period_9 + condition*period_9_sq | pid)
```

526 The specification “0 + Intercept + . . . ” removes the default intercept in brm() and

527 adds an explicit Intercept for which we can set the prior ourselves. The variable

528 period_9_sq is a squared version of period_9. Note that duplicate terms in the model
 529 formula (e.g., condition) are ignored. Because TIME is centered on bin 9, the Intercept
 530 represents the estimated cloglog-hazard in bin 9 for the blank prime condition. Model M1d
 531 took about 184 minutes to run.

532 **4.3.5 Compare the models.** We can compare the three models using the Widely
 533 Applicable Information Criterion (WAIC) and Leave-One-Out (LOO) cross-validation, and
 534 look at model weights for both criteria (Kurz, 2023a; McElreath, 2018).

```
model_weights(model_M0i, model_M1i, model_M1d, weights = "loo") %>% round(digits = 2)
```

535 ## model_M0i model_M1i model_M1d
 536 ## 0 1 0

```
model_weights(model_M0i, model_M1i, model_M1d, weights = "waic") %>% round(digits = 2)
```

537 ## model_M0i model_M1i model_M1d
 538 ## 0 1 0

539 Clearly, both the loo and waic weighting schemes assign a weight of 1 to model M1i,
 540 and a weight of 0 to the other two simpler models.

541 **4.3.6 Interpreting model M1i.** To make inferences from the parameter estimates
 542 in model M1i, we first plot the densities of the draws from the posterior distributions of its
 543 population-level parameters in Figure 5, together with point (median) and interval
 544 estimates (80% and 95% credible intervals).

Posterior distributions for population-level effects in Model M1i

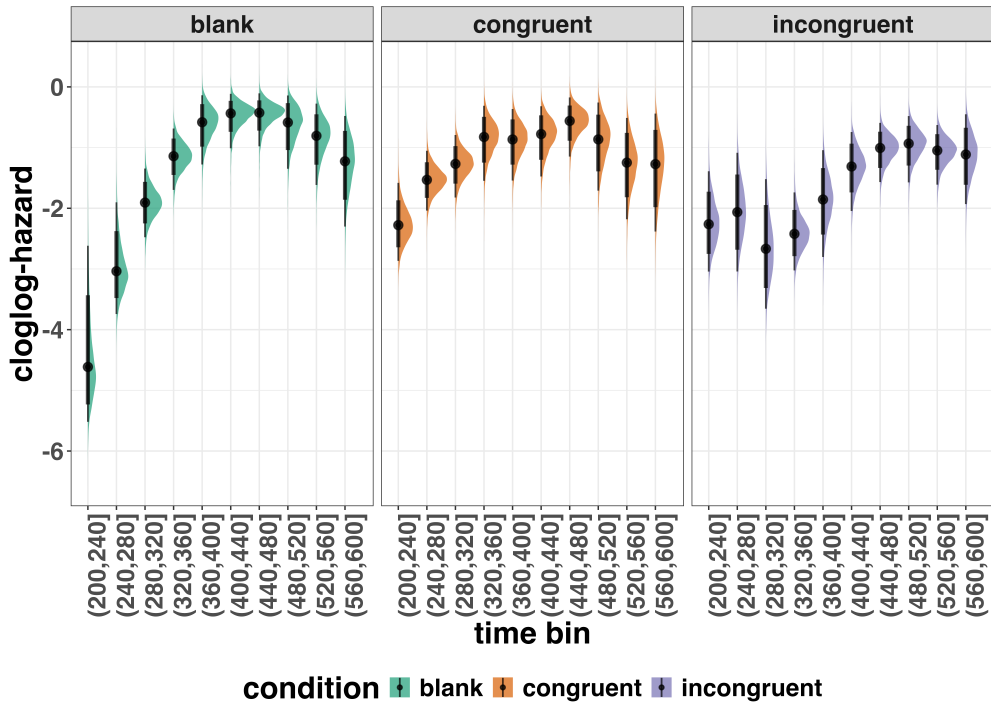


Figure 5. Medians and 80/95% credible intervals of the posterior distributions of the population-level parameters of model M1i.

Because the parameter estimates are on the cloglog-hazard scale, we can ease our

interpretation by plotting the expected value of the posterior predictive distribution – the predicted hazard values – for the average participant (Figure 6), and for each participant in the data set (Figure 7).

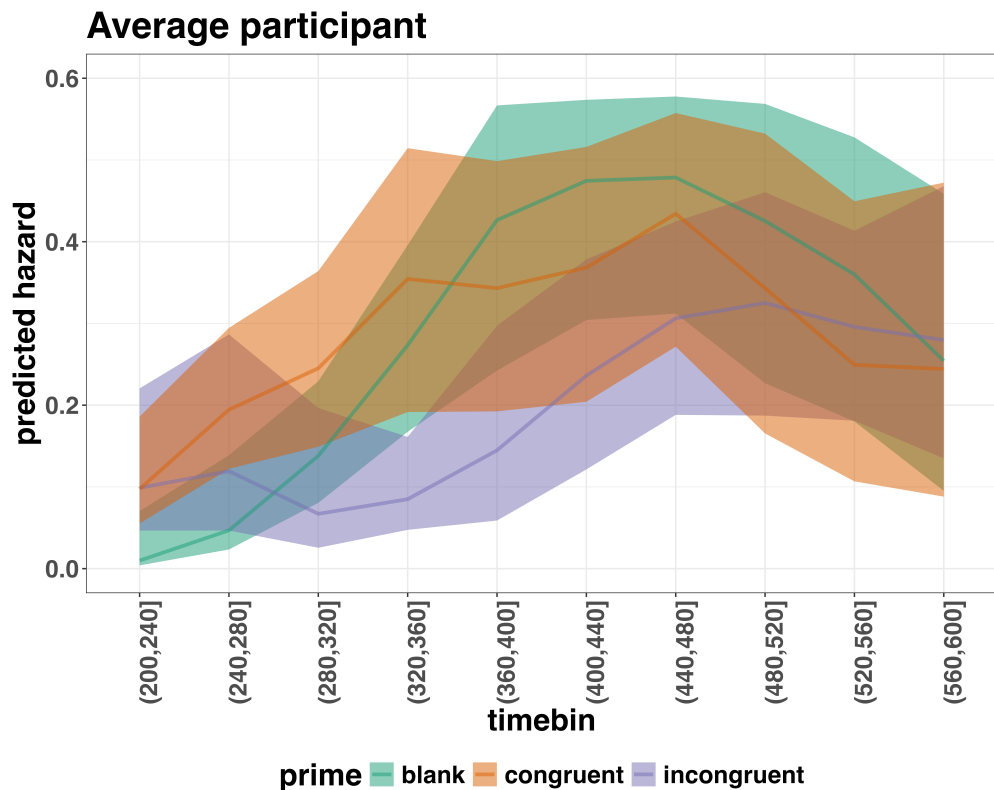


Figure 6. Point (median) and 80/95% credible interval summaries of the hazard estimates (expected values of the draws from the posterior predictive distributions) in each time bin for the average participant.

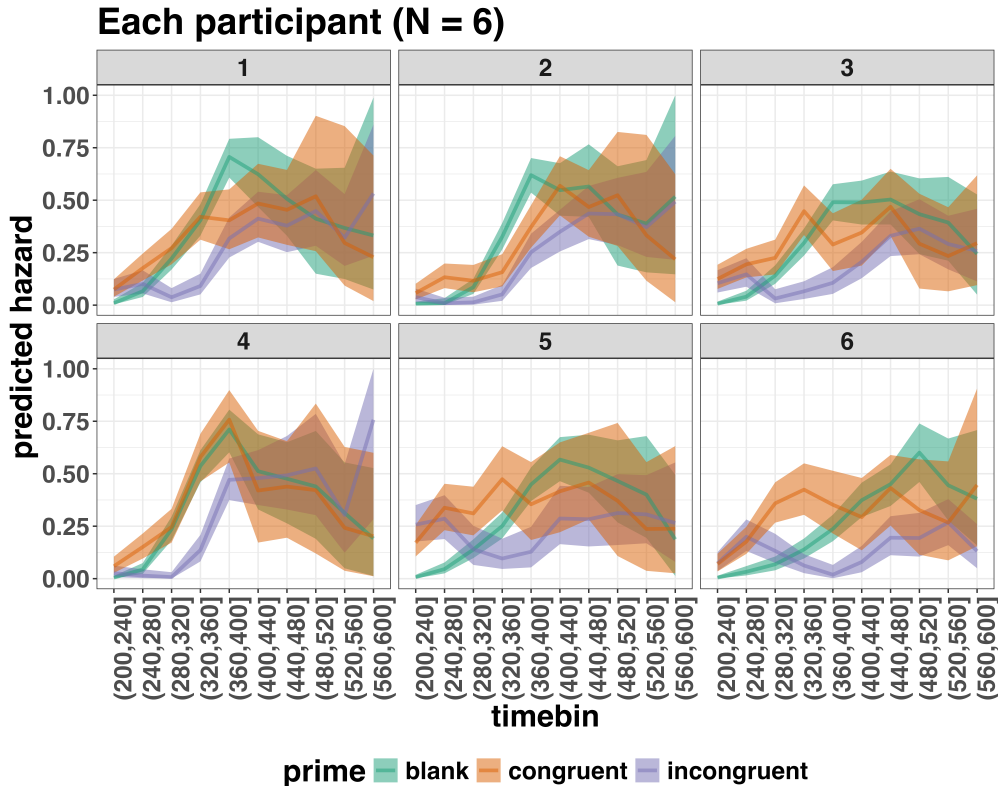


Figure 7. Point (median) and 80/95% credible interval summaries of the hazard estimates (expected values of the draws from the posterior predictive distributions) in each time bin for each participant.

549 As we are actually interested in the effects of congruent and incongruent primes,

550 relative to the blank prime condition, we can construct two contrasts (congruent-blank,

551 incongruent-blank), and plot the posterior distributions of these contrast effects, both for

552 the average participant (Figure 8; grand average marginal effect) and for each participant

553 in the data set (Figure 9; subject-specific average marginal effect).

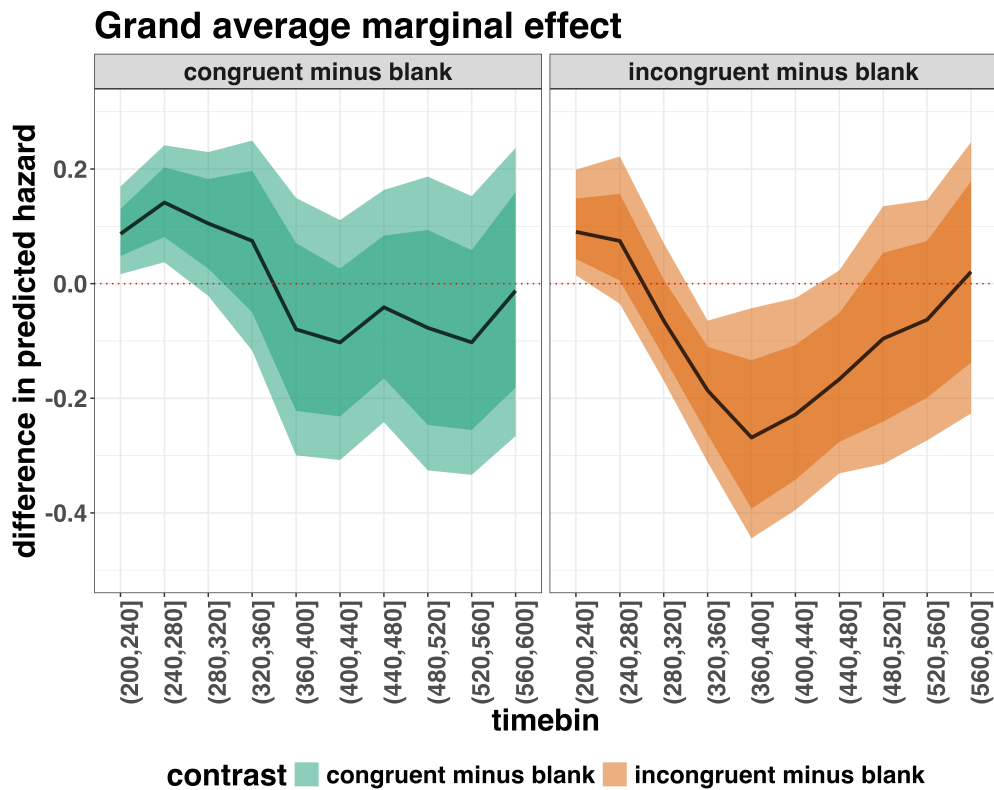


Figure 8. Point (mean) and 80/95% credible interval summaries of estimated differences in hazard in each time bin for the average participant.

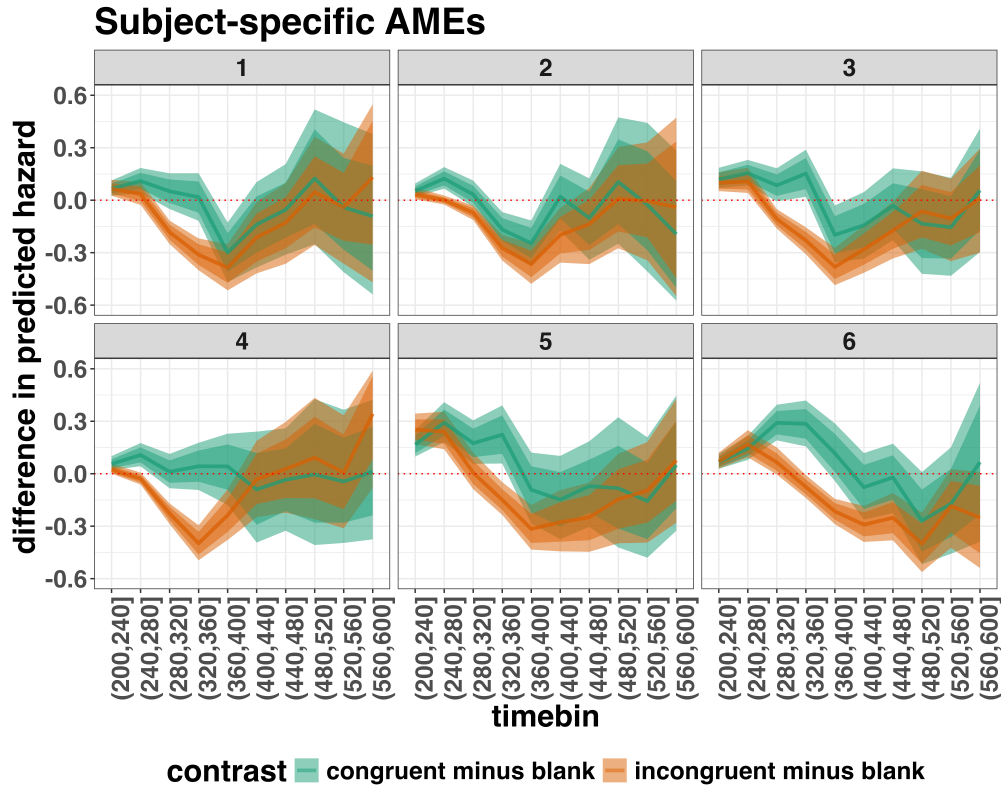


Figure 9. Point (mean) and 80/95% credible interval summaries of estimated differences in hazard in each time bin for each participant.

554 Table 4 shows the summaries of the estimated hazard differences for both contrasts in
 555 terms of a point estimate (the mean) and the upper and lower bounds of the 95% credible
 556 interval, for the average participant.

Table 4

*Point (mean) and 95% credible interval summary of
 estimated differences in hazard, for each time bin and
 contrast, in the average participant.*

contrast	timebin	diff	.lower	.upper
congruent minus blank	6	0.09	0.02	0.17

Table 4 continued

contrast	timebin	diff	.lower	.upper
congruent minus blank	7	0.14	0.04	0.25
congruent minus blank	8	0.11	-0.02	0.24
congruent minus blank	9	0.08	-0.12	0.27
congruent minus blank	10	-0.08	-0.30	0.15
congruent minus blank	11	-0.10	-0.31	0.11
congruent minus blank	12	-0.04	-0.24	0.17
congruent minus blank	13	-0.08	-0.33	0.20
congruent minus blank	14	-0.10	-0.33	0.15
congruent minus blank	15	-0.01	-0.27	0.27
incongruent minus blank	6	0.09	0.01	0.21
incongruent minus blank	7	0.08	-0.03	0.23
incongruent minus blank	8	-0.06	-0.17	0.07
incongruent minus blank	9	-0.19	-0.31	-0.06
incongruent minus blank	10	-0.27	-0.45	-0.04
incongruent minus blank	11	-0.23	-0.40	-0.03
incongruent minus blank	12	-0.17	-0.33	0.02
incongruent minus blank	13	-0.10	-0.31	0.14
incongruent minus blank	14	-0.06	-0.27	0.15
incongruent minus blank	15	0.03	-0.23	0.27

Note. diff = difference in predicted hazard.

558 ***Example conclusions for M1i.*** What can we conclude from model M1i about

559 our research question, i.e., the temporal dynamics of the effect of prime-target congruency
560 on RT? In other words, in which of the 40-ms time bins between 200 and 600 ms after
561 target onset does changing the prime from blank to congruent or incongruent affect the
562 hazard of response occurrence (for a prime-target SOA of 187 ms)?

563 If we want to study the average effect of prime type on hazard, uncontaminated by

564 inter-individual differences, we can base our conclusion on Figure 8 and Table 4. The
565 contrast “congruent minus blank” was estimated to be 0.09 hazard units in bin 6 (95% CrI
566 = [0.02, 0.17]), and 0.14 hazard units in bin 7 (95% CrI = [0.04, 0.25]). For the other bins,
567 the 95% credible interval contained zero. The contrast “incongruent minus blank” was
568 estimated to be 0.09 hazard units in bin 6 (95% CrI = [0.01, 0.21]), -0.19 hazard units in
569 bin 9 (95% CrI = [-0.31, -0.06]), -0.27 hazard units in bin 10 (95% CrI = [-0.45, -0.04]),
570 and -0.23 hazard units in bin 11 (95% CrI = [-0.40, -0.03]). For the other bins, the 95%
571 credible interval contained zero. Note that we could also have calculated hazard ratios
572 instead of hazard differences.

573 There are thus two phases of performance for the average person between 200 and

574 600 ms after target onset. In the first phase, the addition of a congruent or incongruent
575 prime stimulus increases the hazard of response occurrence compared to blank prime trials
576 in the time period (200, 240]. In the second phase, only the incongruent prime decreases
577 the hazard of response occurrence compared to blank primes, in the time period (320,440].
578 The sign of the effect of incongruent primes on the hazard of response occurrence thus
579 depends on how much waiting time has passed since target onset.

580 The posterior distribution of each contrast can also be summarized by considering its

581 proportion below or above some value, like zero. Table 5 shows the proportion of the
582 posterior distribution below or above zero, for each time bin and contrast.

Table 5

Summarizing the posterior distributions of each contrast by their proportion below and above zero.

timebin	contrast	prop_above	prop_below
6	congruent minus blank	0.99	0.01
7	congruent minus blank	0.99	0.01
8	congruent minus blank	0.95	0.05
9	congruent minus blank	0.79	0.21
10	congruent minus blank	0.24	0.76
11	congruent minus blank	0.15	0.85
12	congruent minus blank	0.33	0.67
13	congruent minus blank	0.28	0.72
14	congruent minus blank	0.19	0.81
15	congruent minus blank	0.47	0.53
6	incongruent minus blank	0.98	0.02
7	incongruent minus blank	0.92	0.08
8	incongruent minus blank	0.12	0.88
9	incongruent minus blank	0.00	1.00
10	incongruent minus blank	0.01	0.99
11	incongruent minus blank	0.02	0.98
12	incongruent minus blank	0.04	0.96
13	incongruent minus blank	0.20	0.80
14	incongruent minus blank	0.27	0.73
15	incongruent minus blank	0.58	0.42

Note. prop_below = proportion below zero; prop_above = proportion above zero.

583

584 Thus, the probability that the contrast “congruent minus blank” is larger than 0, is
585 larger than .9 in bins 6 to 8. And the probability that the contrast “incongruent minus
586 blank” is smaller than 0, is larger than .9 in bins 9 to 12.

587 If we want to focus more on inter-individual differences, we can study the
588 subject-specific hazard functions in Figure 9. Note that three participants (1, 2, and 3)
589 show a negative difference for the contrast “congruent minus incongruent” in bin (360,400]
590 – subject 2 also in bin (320,360].

591 Future studies could (a) increase the number of participants to estimate the
592 proportion of “dippers” in the subject population, and/or (b) try to explain why this dip
593 occurs. For example, Panis and Schmidt (2016) concluded that active, top-down,
594 task-guided response inhibition effects emerge around 360 ms after the onset of the
595 stimulus following the prime (here: the target stimulus). Such a top-down inhibitory effect
596 might exist in our priming data set, because after some time participants will learn that the
597 first stimulus is not the one they have to respond to; To prevent a premature overt response
598 to the prime they thus might gradually increase a global response threshold during the
599 remainder of the experiment, which could result in a lower hazard in congruent trials
600 compared to blank trials, for bins after ~360 ms, and towards the end of the experiment.
601 This effect might be masked for incongruent primes by the response competition effect.

602 Interestingly, all subjects show a tendency in their mean difference (congruent minus
603 blank) to “dip” around that time (Figure 9). Therefore, future modeling efforts could
604 incorporate the trial number into the model formula, in order to also study how the effects
605 of prime type on hazard change on the long experiment-wide time scale, next to the short
606 trial-wide time scale. In Tutorial_2a.Rmd we provide a number of model formula that
607 should get you going.

608 **4.4 Tutorial 2b: Fitting Bayesian conditional accuracy models**

609 In this fourth tutorial, we illustrate how to fit a Bayesian multi-level regression model
 610 to the timed accuracy data from the masked response priming data set used in Tutorial 1a.

611 The general process is similar to Tutorial 2a, except that (a) we use the person-trial data
 612 set, (b) we use the logit link function, and (c) we change the priors. To keep the tutorial
 613 short, we only fitted the effects of model M1i (see Tutorial 2a) in the conditional accuracy
 614 model called M1i_ca.

615 To make inferences from the parameter estimates in model M1i_ca, we first plot the
 616 densities of the draws from the posterior distributions of its population-level parameters in
 617 Figure 10, together with point (median) and interval estimates (80% and 95% credible
 618 intervals).

**Posterior distributions for population-level
effects in Model M1i_ca**

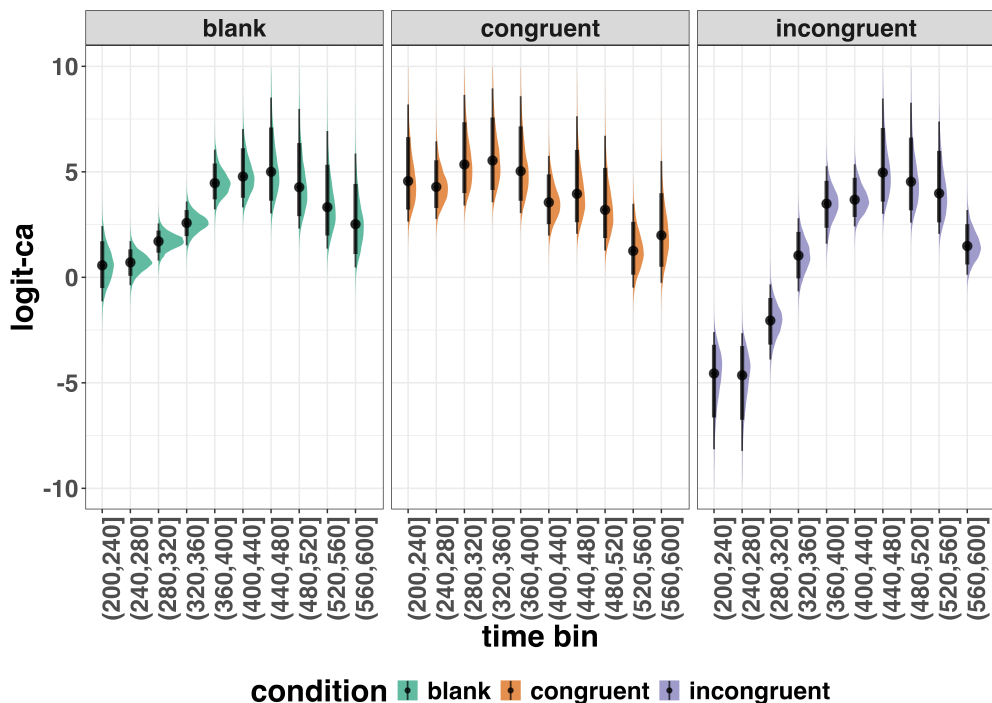


Figure 10. Medians and 80/95% credible intervals of the posterior distributions of the population-level parameters of model M1i_ca.

619 Because the parameter estimates are on the logit-ca scale, we can ease our
 620 interpretation by plotting the expected value of the posterior predictive distribution – the
 621 predicted conditional accuracies – for the average participant (Figure 11), and for each
 622 participant in the data set (Figure 12).

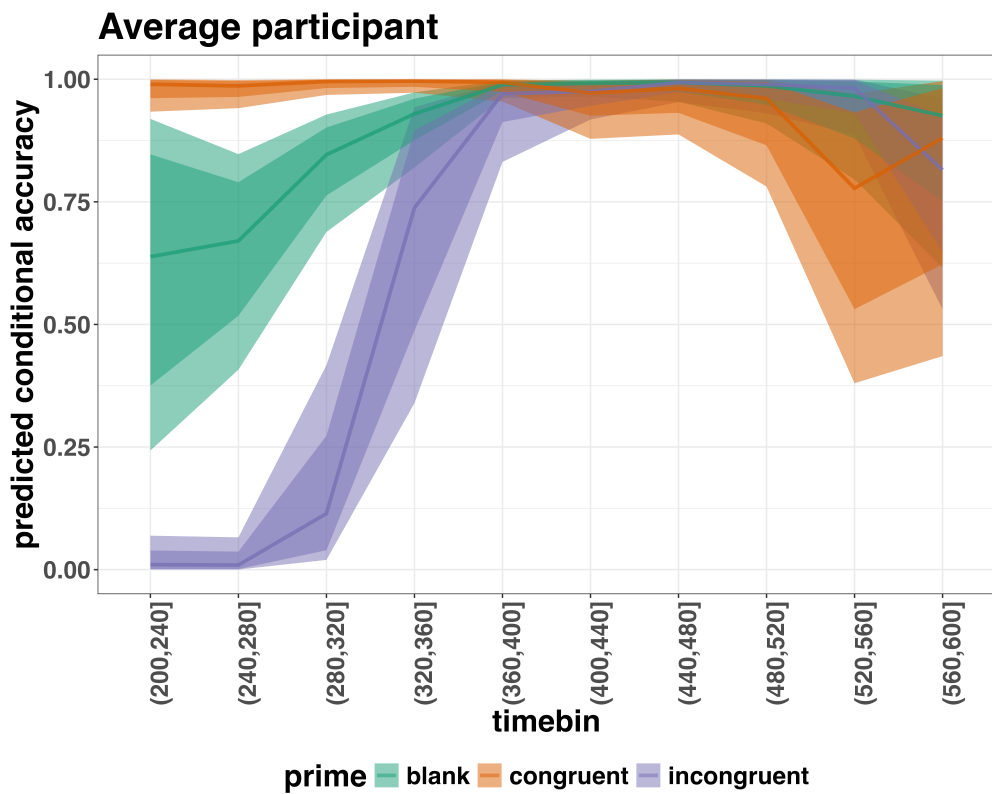


Figure 11. Point (median) and 80/95% credible interval summaries of the conditional accuracy estimates (expected values of the draws from the posterior predictive distributions) in each time bin for the average participant.

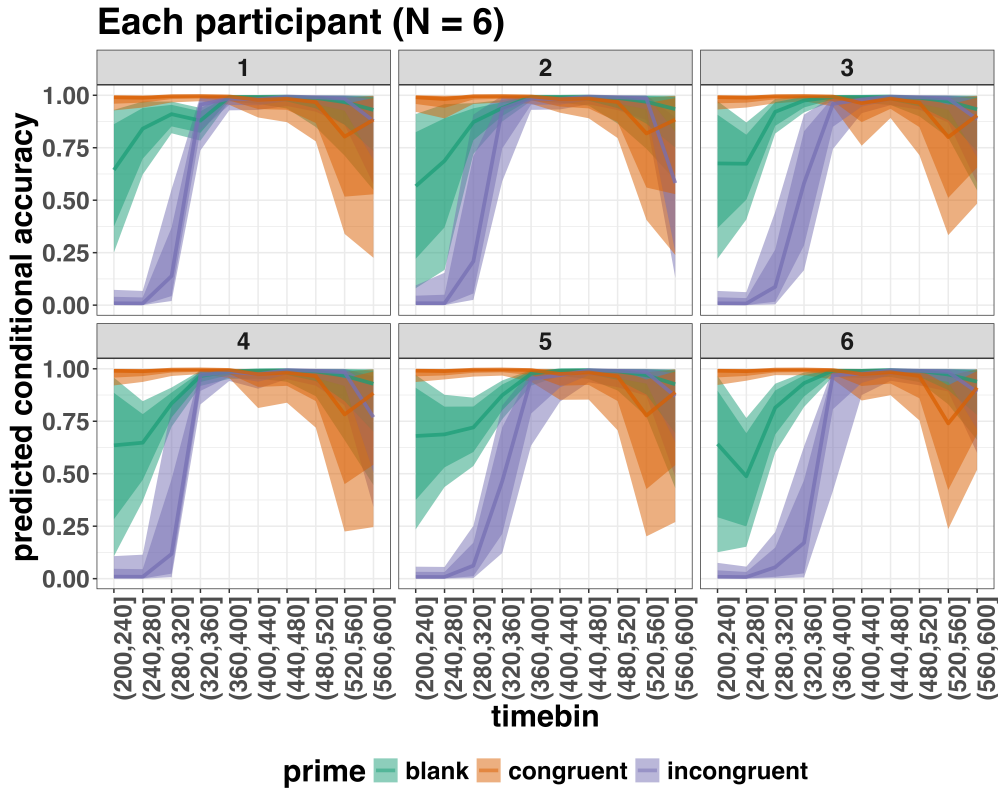


Figure 12. Point (median) and 80/95% credible interval summaries of the conditional accuracy estimates (expected values of the draws from the posterior predictive distributions) in each time bin for each participant.

As we are actually interested in the effects of congruent and incongruent primes,

relative to the blank prime condition, we can construct two contrasts (congruent-blank,

incongruent-blank), and plot the posterior distributions of these contrast effects for the

average participant (Figure 13; grand average marginal effect).

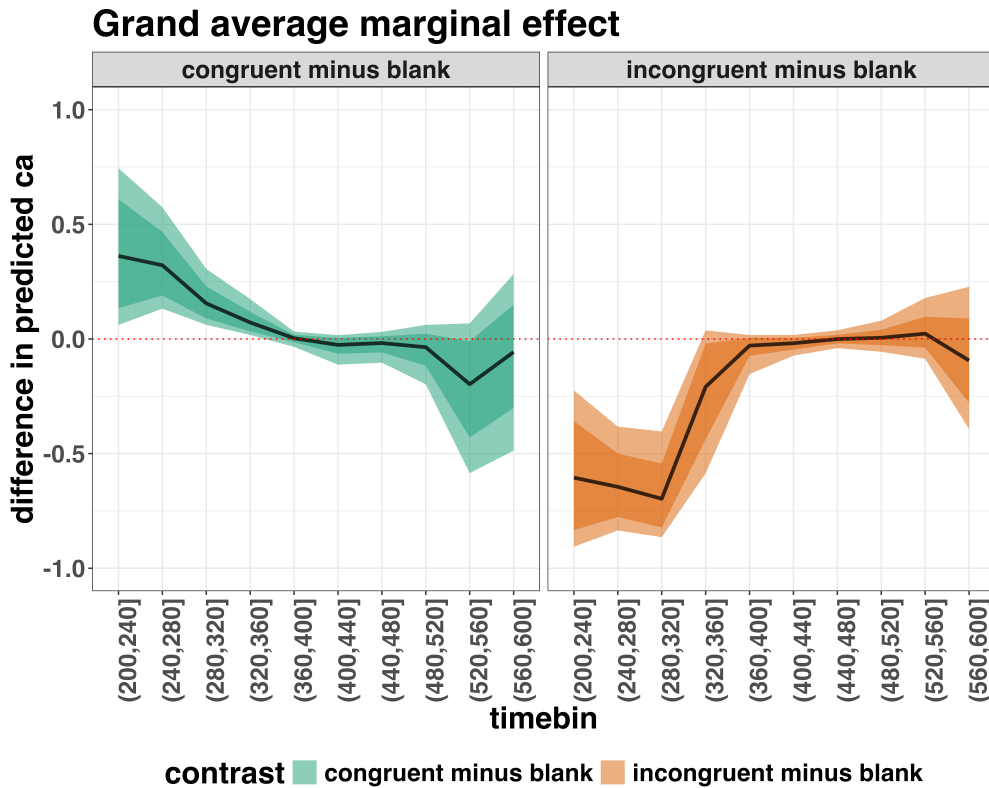


Figure 13. Point (mean) and 80/95% credible interval summaries of estimated differences in conditional accuracy in each time bin for the average participant.

627 Table 6 shows the summaries of the estimated differences in conditional accuracy for
 628 both contrasts in terms of a point estimate (the mean) and the upper and lower bounds of
 629 the 95% credible interval, for the average participant.

Table 6

Point (mean) and 95% credible interval summary of estimated differences in conditional accuracy, for each time bin and contrast, in the average participant.

contrast	timebin	diff_ca	.lower	.upper
congruent minus blank	6	0.36	0.06	0.74

Table 6 continued

contrast	timebin	diff_ca	.lower	.upper
congruent minus blank	7	0.32	0.13	0.57
congruent minus blank	8	0.16	0.06	0.31
congruent minus blank	9	0.07	0.02	0.17
congruent minus blank	10	0.00	-0.03	0.03
congruent minus blank	11	-0.03	-0.11	0.02
congruent minus blank	12	-0.02	-0.10	0.03
congruent minus blank	13	-0.04	-0.20	0.06
congruent minus blank	14	-0.20	-0.59	0.07
congruent minus blank	15	-0.06	-0.49	0.28
incongruent minus blank	6	-0.61	-0.91	-0.22
incongruent minus blank	7	-0.64	-0.84	-0.38
incongruent minus blank	8	-0.70	-0.86	-0.40
incongruent minus blank	9	-0.21	-0.59	0.04
incongruent minus blank	10	-0.03	-0.15	0.02
incongruent minus blank	11	-0.02	-0.07	0.02
incongruent minus blank	12	0.00	-0.04	0.04
incongruent minus blank	13	0.01	-0.06	0.08
incongruent minus blank	14	0.02	-0.09	0.18
incongruent minus blank	15	-0.09	-0.39	0.23

Note. diff = difference in predicted conditional accuracy.

632 on the conditional accuracy of emitted responses in time bins (200,240], (240,280], and
633 (280,320], relative to the estimates in the baseline condition (blank prime; red dashed lines
634 in Figure 14). Incongruent primes have a negative effect on the conditional accuracy of
635 emitted responses in those time bins, relative to the estimates in the baseline condition.

636 **4.5 Tutorial 3a: Fitting Frequentist hazard models**

637 In this fifth tutorial we illustrate how to fit a multilevel regression model to RT data
638 in the frequentist framework, for the data set used in Tutorial 1a. The general process is
639 similar to that in Tutorial 2a, except that there are no priors to set.

640 To keep this tutorial short, we only fitted the effects from model M1i (see Tutorial
641 2a) using the function `glmer()` from the R package `lme4`. Alternatively, one could also use
642 the function `glmmPQL()` from the R package `MASS` (Ripley et al., 2024). The resulting
643 hazard model is called `M1i_f`.

644 In Figure 14 we compare the parameter estimates of model M1i from `brm()` with
645 those of model `M1i_f` from `glmer()`.

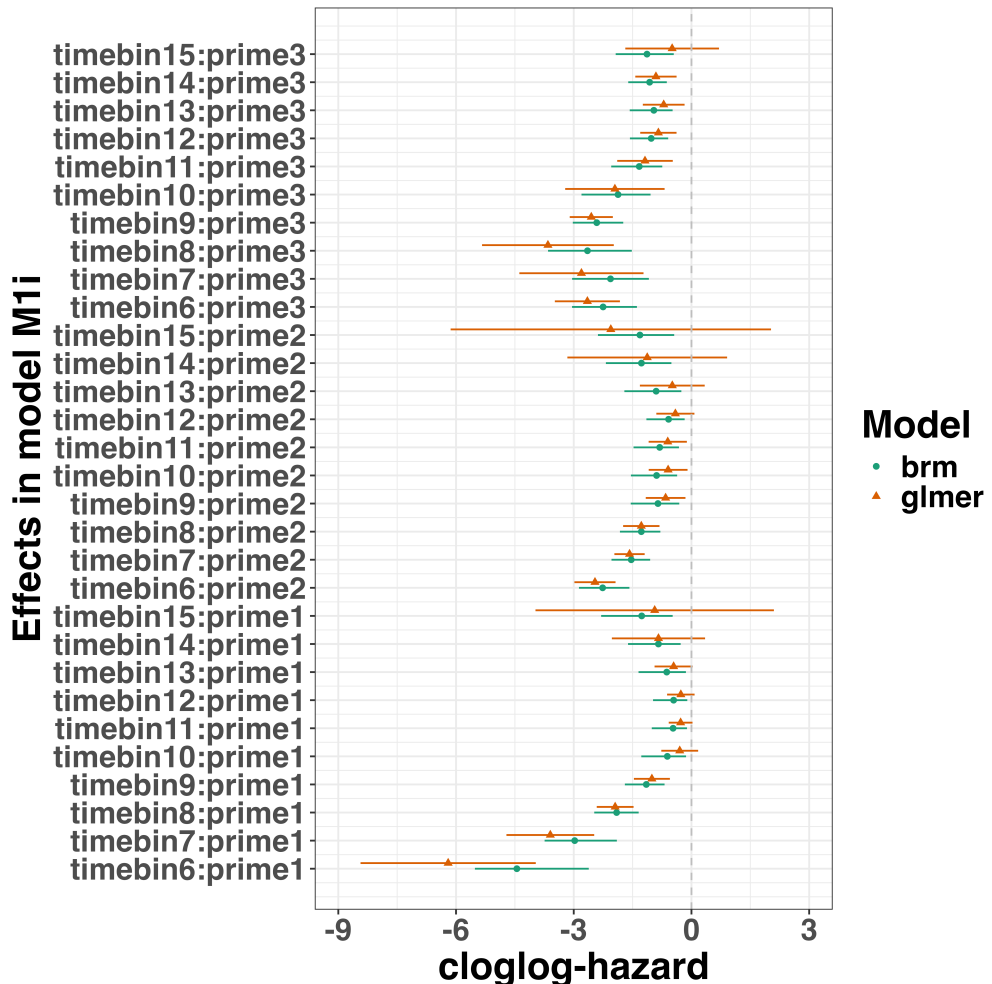


Figure 14. Parameter estimates for model M1i from `brm()` – means and 95% credible intervals – and model M1i_f from `glmer()` – maximum likelihood estimates and 95% confidence intervals.

646 Figure 14 confirms that the parameter estimates from both Bayesian and frequentist

647 models are pretty similar, which makes sense given the close similarity in model structure.

648 However, model M1i_f did not converge and resulted in a singular fit. This is of course one

649 of the reasons why Bayesian modeling has become so popular in recent years. But the price

650 you pay for being able to fit more complex random effects models in a Bayesian framework

651 is computation time. In other words, as we have noted throughout, some of the Bayesian

652 models in Tutorials 2a took several hours to build.

653 4.6 Tutorial 3b: Fitting Frequentist conditional accuracy models

654 In this sixth tutorial we illustrate how to fit a multilevel regression model to the
655 timed accuracy data in the frequentist framework, for the data set used in Tutorial 1a. To
656 keep it short, we only fitted the effects from model M1i_ca (see Tutorial 2b) using the
657 function glmer() from the R package lme4. Alternatively, one could also use the function
658 glmmPQL() from the R package MASS (Ripley et al., 2024). Again, the resulting
659 conditional accuracy model M1i_ca_f did not converge and resulted in a singular fit.

660 4.4 Tutorial 4: Planning

661 This needs adding... RR to do this.

662 5. Discussion

663 This main motivation for writing this paper is the observation that EHA and SAT
664 analysis remain under-used in psychological research. As a consequence, the field of
665 psychological research is not taking full advantage of the many benefits EHA/SAT provides
666 compared to more conventional analyses. By providing a freely available set of tutorials,
667 which provide step-by-step guidelines and ready-to-use R code, we hope that researchers
668 will feel more comfortable using EHA/SAT in the future. Indeed, we hope that our
669 tutorials may help to overcome a barrier to entry with EHA/SAT, which is that such
670 approaches require more analytical complexity compared to mean-average comparisons.
671 While we have focused here on within-subject, factorial, small- N designs, it is important to
672 realize that EHA/SAT can be applied to other designs as well (large- N designs with only
673 one measurement per subject, between-subject designs, etc.). As such, the general workflow
674 and associated code can be modified and applied more broadly to other contexts and
675 research questions. In the following, we discuss issues relating to model complexity and

676 interpretability, individual differences, as well as limitations of the approach and future
677 extensions.

678 **5.1 What are the main use-cases of EHA for understanding cognition and brain
679 function?**

680 For those researchers, like ourselves, who are primarily interested in understanding
681 human cognitive and brain systems, we consider two broadly-defined, main use-cases of
682 EHA. First, as we hope to have made clear by this point, EHA is one way to investigating
683 a “temporal states” approach to cognitive processes. EHA provides one way to uncover
684 when cognitive states may start and stop, as well as what they may be tied to or interact
685 with. Therefore, if your research questions concern **when** and **for how long** psychological
686 states occur, our EHA tutorials could be useful tools for you to use.

687 Second, even if you are not primarily interested in studying the temporal states of
688 cognition, EHA could still be a useful tool to consider using, in order to qualify inferences
689 that are being made based on mean-average comparisons. Given that distinctly different
690 inferences can be made from the same data based on whether one computes a
691 mean-average across trials or a RT distribution of events (Figure 1), it may be important
692 for researchers to supplement mean-average comparisons with EHA. One could envisage
693 scenarios where the implicit assumption of an effect manifesting across all of the time bins
694 measured would not be supported by EHA. Therefore, the conclusion of interest would not
695 apply to all responses, but instead it would be restricted to certain aspects of time.

696 **5.2 Model complexity versus interpretability**

697 EHA can quickly become very complex when adding more than 1 time scale, due to
698 the many possible higher-order interactions. For example, some of the models discussed in
699 Tutorial 2a (M2) contain two time scales as covariates: the passage of time on the

700 within-trial time scale, and the passage of time on the across-trial (or within-experiment)
701 time scale. However, when trials are presented in blocks, and blocks of trials within
702 sessions, and when the experiment comprises three sessions, then four time scales can be
703 defined (within-trial, within-block, within-session, and within-experiment). From a
704 theoretical perspective, adding more than 1 time scale – and their interactions – can be
705 important to capture plasticity and other learning effects that may play out on such longer
706 time scales, and that are probably present in each experiment in general. From a practical
707 perspective, therefore, some choices need to be made to balance the amount of data that is
708 being collected per participant, condition and across the varying timescales. As one
709 example, if there are several timescales of relevance, then it might be prudent for
710 interpretational purposes to limit the number of experimental predictor variables
711 (conditions). This is of course where planning and data simulation efforts would be
712 important to provide a guide to experimental design choices (see Tutorial 4).

713 5.3 Individual differences

714 One important issue is that of possible individual differences in the overall location of
715 the distribution, and the time course of psychological effects. For example, when you wait
716 for a response of the participant on each trial, you allow the participant to have control
717 over the trial duration, and some participants might respond only when they are confident
718 that their emitted response will be correct. These issues can be avoided by introducing a
719 (relatively short) response deadline in each trial, e.g., 600 ms for simple detection tasks,
720 1000 ms for more difficult discrimination tasks, or 2 s for tasks requiring extended high-level
721 processing. Because EHA can deal in a straightforward fashion with right-censored
722 observations (i.e., trials without an observed response), introducing a response deadline is
723 recommended when designing RT experiments. Furthermore, introducing a response
724 deadline and asking participants to respond before the deadline as much as possible, will
725 also lead to individual distributions that overlap in time, which is important when selecting

726 a common analysis time window when fitting hazard and conditional accuracy models.

727 But even when using a response deadline, participants can differ qualitatively in the
728 effects they display (see Panis, 2020). One way to deal with this is to describe and
729 interpret the different patterns. Another way is to run a clustering algorithm on the
730 individual hazard estimates across all conditions. The obtained dendrogram can then be
731 used to identify a (hopefully big) cluster of participants that behave similarly, and to
732 identify a (hopefully small) cluster of participants with different behavioral patterns. One
733 might then exclude the smaller sub-group of participants before fitting a hazard model or
734 consider the possibility that different cognitive processes may be at play during task
735 performance across the different sub-groups.

736 Another approach to deal with individual differences is Bayesian prevalence (Ince,
737 Paton, Kay, & Schyns, 2021), which is a from of Small-N approach (Smith & Little, 2018).
738 This method looks at effects within each individual in the study and asks how likely it
739 would be to see the same result if the experiment was repeated with a new person chosen
740 from the wider population at random. This approach allows one to quantify how typical or
741 uncommon an observed effect is in the population, and the uncertainty around this
742 estimate.

743 5.4 Limitations

744 Compared to the orthodox method – comparing mean-averages between conditions –
745 the most important limitation of multi-level hazard and conditional accuracy modeling is
746 that it might take a long time to estimate the parameters using Bayesian methods or the
747 model might have to be simplified significantly to use frequentist methods.

748 Another issue is that you need a relatively large number of trials per condition to
749 estimate the hazard function with high temporal resolution, which is required when testing
750 predictions of process models of cognition. Indeed, in general, there is a trade-off between

751 the number of trials per condition and the temporal resolution (i.e., bin width) of the
752 hazard function. Therefore, we recommend researchers to collect as many trials as possible
753 per experimental condition, given the available resources and considering the participant
754 experience (e.g., fatigue and boredom). For instance, if the maximum session length
755 deemed reasonable is between 1 and 2 hours, what is the maximum number of trials per
756 condition that you could reasonably collect? After consideration, it might be worth
757 conducting multiple testing sessions per participant and/or reducing the number of
758 experimental conditions. Finally, there is a user-friendly online tool for calculating
759 statistical power as a function of the number of trials as well as the number of participants,
760 and this might be worth consulting to guide the research design process (Baker et al., 2021).

761 We did not discuss continuous-time EHA, nor continuous-time SAT analysis. As
762 indicated by Allison (2010), learning discrete-time EHA methods first will help in learning
763 continuous-time methods. Given that RT is typically treated as a continuous variable, it is
764 possible that continuous-time methods will ultimately prevail. However, they require much
765 more data to estimate the continuous-time hazard (rate) function well. Thus, by trading a
766 bit of temporal resolution for a lower number of trials, discrete-time methods seem ideal for
767 dealing with typical psychological time-to-event data sets for which there are less than
768 ~200 trials per condition per experiment.

769 5.5 Extensions

770 The hazard models in this tutorial assume that there is one event of interest. For RT
771 data, this event constitutes a single transition between an “idle” state and a “responded”
772 state. However, in certain situations, more than one event of interest might exist. For
773 example, in a medical or health-related context, an individual might transition back and
774 forth between a “healthy” state and a “depressed” state, before being absorbed into a final
775 “death” state. When you have data on the timing of these transitions, one can apply
776 multi-state hazard models, which generalize EHA to transitions between three or more

777 states (Steele, Goldstein, & Browne, 2004). Also, the predictor variables in this tutorial are
778 time-invariant, i.e., their value did not change over the course of a trial. Thus, another
779 extension is to include time-varying predictors, i.e., predictors whose value can change
780 across the time bins within a trial (Allison, 2010). For example, when gaze position is
781 tracked during a visual search trial, the gaze-target distance will vary during a trial when
782 the eyes move around before a manual response is given; shorter gaze-target distances
783 should be associated with a higher hazard of response occurrence. Note that the effect of a
784 time-varying predictor (e.g., an occipital EEG signal) can itself vary over time.

785 **6. Conclusions**

786 Estimating the temporal distributions of RT and accuracy provide a rich source of
787 information on the time course of cognitive processing, which have been largely
788 undervalued in the history of experimental psychology and cognitive neuroscience.
789 Statistically controlling for the passage of time during data analysis is equally important as
790 experimental control during the design of an experiment, to better understand human
791 behavior in experimental paradigms. We hope that by providing a set of hands-on,
792 step-by-step tutorials, which come with custom-built and freely available code, researchers
793 will feel more comfortable embracing EHA and investigating the temporal profile of
794 cognitive states. On a broader level, we think that wider adoption of such approaches will
795 have a meaningful impact on the inferences drawn from data, as well as the development of
796 theories regarding the structure of cognition.

797

References

- 798 Allison, P. D. (1982). Discrete-Time Methods for the Analysis of Event Histories.
799 *Sociological Methodology*, 13, 61. <https://doi.org/10.2307/270718>
- 800 Allison, P. D. (2010). *Survival analysis using SAS: A practical guide* (2. ed). Cary, NC:
801 SAS Press.
- 802 Aust, F. (2019). *Citr: 'RStudio' add-in to insert markdown citations*. Retrieved from
803 <https://github.com/crsh/citr>
- 804 Aust, F., & Barth, M. (2023). *papaja: Prepare reproducible APA journal articles with R*
805 *Markdown*. Retrieved from <https://github.com/crsh/papaja>
- 806 Aust, F., & Barth, M. (2024). *papaja: Prepare reproducible APA journal articles with R*
807 *Markdown*. <https://doi.org/10.32614/CRAN.package.papaja>
- 808 Baker, D. H., Vilidaite, G., Lygo, F. A., Smith, A. K., Flack, T. R., Gouws, A. D., &
809 Andrews, T. J. (2021). Power contours: Optimising sample size and precision in
810 experimental psychology and human neuroscience. *Psychological Methods*, 26(3),
811 295–314. <https://doi.org/10.1037/met0000337>
- 812 Barr, D. J., Levy, R., Scheepers, C., & Tily, H. J. (2013). Random effects structure for
813 confirmatory hypothesis testing: Keep it maximal. *Journal of Memory and Language*,
814 68(3), 10.1016/j.jml.2012.11.001. <https://doi.org/10.1016/j.jml.2012.11.001>
- 815 Barth, M. (2023). *tinylabes: Lightweight variable labels*. Retrieved from
816 <https://cran.r-project.org/package=tinylabes>
- 817 Bates, D., Mächler, M., Bolker, B., & Walker, S. (2015). Fitting linear mixed-effects
818 models using lme4. *Journal of Statistical Software*, 67(1), 1–48.
819 <https://doi.org/10.18637/jss.v067.i01>
- 820 Bates, D., Maechler, M., & Jagan, M. (2024). *Matrix: Sparse and dense matrix classes and*
821 *methods*. Retrieved from <https://CRAN.R-project.org/package=Matrix>
- 822 Bengtsson, H. (2021). A unifying framework for parallel and distributed processing in r
823 using futures. *The R Journal*, 13(2), 208–227. <https://doi.org/10.32614/RJ-2021-048>

- 824 Blossfeld, H.-P., & Rohwer, G. (2002). *Techniques of event history modeling: New*
825 *approaches to causal analysis, 2nd ed* (pp. x, 310). Mahwah, NJ, US: Lawrence
826 Erlbaum Associates Publishers.
- 827 Box-Steffensmeier, J. M. (2004). Event history modeling: A guide for social scientists.
828 Cambridge: University Press.
- 829 Bürkner, P.-C. (2017). brms: An R package for Bayesian multilevel models using Stan.
830 *Journal of Statistical Software*, 80(1), 1–28. <https://doi.org/10.18637/jss.v080.i01>
- 831 Bürkner, P.-C. (2018). Advanced Bayesian multilevel modeling with the R package brms.
832 *The R Journal*, 10(1), 395–411. <https://doi.org/10.32614/RJ-2018-017>
- 833 Bürkner, P.-C. (2021). Bayesian item response modeling in R with brms and Stan. *Journal*
834 *of Statistical Software*, 100(5), 1–54. <https://doi.org/10.18637/jss.v100.i05>
- 835 Eddelbuettel, D., & Balamuta, J. J. (2018). Extending R with C++: A Brief Introduction
836 to Rcpp. *The American Statistician*, 72(1), 28–36.
837 <https://doi.org/10.1080/00031305.2017.1375990>
- 838 Eddelbuettel, D., & François, R. (2011). Rcpp: Seamless R and C++ integration. *Journal*
839 *of Statistical Software*, 40(8), 1–18. <https://doi.org/10.18637/jss.v040.i08>
- 840 Gabry, J., Češnovar, R., Johnson, A., & Brodner, S. (2024). *Cmdstanr: R interface to*
841 *'CmdStan'*. Retrieved from <https://github.com/stan-dev/cmdstanr>
- 842 Gabry, J., Simpson, D., Vehtari, A., Betancourt, M., & Gelman, A. (2019). Visualization
843 in bayesian workflow. *J. R. Stat. Soc. A*, 182, 389–402.
844 <https://doi.org/10.1111/rssa.12378>
- 845 Gelman, A., Hill, J., & Vehtari, A. (2020). Regression and Other Stories.
846 [https://www.cambridge.org/highereducation/books/regression-and-other-](https://www.cambridge.org/highereducation/books/regression-and-other-stories/DD20DD6C9057118581076E54E40C372C)
847 [stories/DD20DD6C9057118581076E54E40C372C](https://www.cambridge.org/highereducation/books/regression-and-other-stories/DD20DD6C9057118581076E54E40C372C); Cambridge University Press.
848 <https://doi.org/10.1017/9781139161879>
- 849 Gelman, A., Vehtari, A., Simpson, D., Margossian, C. C., Carpenter, B., Yao, Y., ...
850 Modrák, M. (2020). *Bayesian Workflow*. arXiv.

- 851 https://doi.org/10.48550/arXiv.2011.01808
- 852 Girard, J. (2024). *Standist: What the package does (one line, title case)*. Retrieved from
853 https://github.com/jmgirard/standist
- 854 Gromelund, G., & Wickham, H. (2011). Dates and times made easy with lubridate.
855 *Journal of Statistical Software*, 40(3), 1–25. Retrieved from
856 https://www.jstatsoft.org/v40/i03/
- 857 Halley, E. (1997). VI. An estimate of the degrees of the mortality of mankind; drawn from
858 curious tables of the births and funerals at the city of Breslaw; with an attempt to
859 ascertain the price of annuities upon lives. *Philosophical Transactions of the Royal
Society of London*, 17(196), 596–610. https://doi.org/10.1098/rstl.1693.0007
- 860
- 861 Heiss, A. (2021, November 10). A Guide to Correctly Calculating Posterior Predictions
862 and Average Marginal Effects with Multilevel Bayesian Models.
863 https://doi.org/10.59350/wbn93-edb02
- 864 Holden, J. G., Van Orden, G. C., & Turvey, M. T. (2009). Dispersion of response times
865 reveals cognitive dynamics. *Psychological Review*, 116(2), 318–342.
866 https://doi.org/10.1037/a0014849
- 867 Hosmer, D. W., Lemeshow, S., & May, S. (2011). *Applied Survival Analysis: Regression
868 Modeling of Time to Event Data* (2nd ed). Hoboken: John Wiley & Sons.
- 869 Ince, R. A., Paton, A. T., Kay, J. W., & Schyns, P. G. (2021). Bayesian inference of
870 population prevalence. *eLife*, 10, e62461. https://doi.org/10.7554/eLife.62461
- 871 Kantowitz, B. H., & Pachella, R. G. (2021). The Interpretation of Reaction Time in
872 Information-Processing Research 1. *Human Information Processing*, 41–82.
873 https://doi.org/10.4324/9781003176688-2
- 874 Kay, M. (2023). *tidybayes: Tidy data and geoms for Bayesian models*.
875 https://doi.org/10.5281/zenodo.1308151
- 876 Kelso, J. A. S., Dumas, G., & Tognoli, E. (2013). Outline of a general theory of behavior
877 and brain coordination. *Neural Networks: The Official Journal of the International*

- 878 *Neural Network Society*, 37, 120–131. <https://doi.org/10.1016/j.neunet.2012.09.003>
- 879 Kruschke, J. K., & Liddell, T. M. (2018). The Bayesian New Statistics: Hypothesis testing,
880 estimation, meta-analysis, and power analysis from a Bayesian perspective.
- 881 *Psychonomic Bulletin & Review*, 25(1), 178–206.
882 <https://doi.org/10.3758/s13423-016-1221-4>
- 883 Kurz, A. S. (2023a). *Applied longitudinal data analysis in brms and the tidyverse* (version
884 0.0.3). Retrieved from <https://bookdown.org/content/4253/>
- 885 Kurz, A. S. (2023b). *Statistical rethinking with brms, ggplot2, and the tidyverse: Second
886 edition* (version 0.4.0). Retrieved from <https://bookdown.org/content/4857/>
- 887 Landes, J., Engelhardt, S. C., & Pelletier, F. (2020). An introduction to event history
888 analyses for ecologists. *Ecosphere*, 11(10), e03238. <https://doi.org/10.1002/ecs2.3238>
- 889 Luce, R. D. (1991). *Response times: Their role in inferring elementary mental organization*
890 (1. issued as paperback). Oxford: Univ. Press.
- 891 Makeham, William M. (1860). *On the Law of Mortality and the Construction of Annuity
892 Tables*. The Assurance Magazine, and Journal of the Institute of Actuaries.
- 893 McElreath, R. (2018). *Statistical Rethinking: A Bayesian Course with Examples in R and
894 Stan* (1st ed.). Chapman and Hall/CRC. <https://doi.org/10.1201/9781315372495>
- 895 Meyer, D. E., Osman, A. M., Irwin, D. E., & Yantis, S. (1988). Modern mental
896 chronometry. *Biological Psychology*, 26(1-3), 3–67.
897 [https://doi.org/10.1016/0301-0511\(88\)90013-0](https://doi.org/10.1016/0301-0511(88)90013-0)
- 898 Müller, K., & Wickham, H. (2023). *Tibble: Simple data frames*. Retrieved from
899 <https://CRAN.R-project.org/package=tibble>
- 900 Neuwirth, E. (2022). *RColorBrewer: ColorBrewer palettes*. Retrieved from
901 <https://CRAN.R-project.org/package=RColorBrewer>
- 902 Panis, S. (2020). How can we learn what attention is? Response gating via multiple direct
903 routes kept in check by inhibitory control processes. *Open Psychology*, 2(1), 238–279.
904 <https://doi.org/10.1515/psych-2020-0107>

- 905 Panis, S., Moran, R., Wolkersdorfer, M. P., & Schmidt, T. (2020). Studying the dynamics
906 of visual search behavior using RT hazard and micro-level speed–accuracy tradeoff
907 functions: A role for recurrent object recognition and cognitive control processes.
908 *Attention, Perception, & Psychophysics*, 82(2), 689–714.
909 <https://doi.org/10.3758/s13414-019-01897-z>
- 910 Panis, S., Schmidt, F., Wolkersdorfer, M. P., & Schmidt, T. (2020). Analyzing Response
911 Times and Other Types of Time-to-Event Data Using Event History Analysis: A Tool
912 for Mental Chronometry and Cognitive Psychophysiology. *I-Perception*, 11(6),
913 2041669520978673. <https://doi.org/10.1177/2041669520978673>
- 914 Panis, S., & Schmidt, T. (2016). What Is Shaping RT and Accuracy Distributions? Active
915 and Selective Response Inhibition Causes the Negative Compatibility Effect. *Journal of*
916 *Cognitive Neuroscience*, 28(11), 1651–1671. https://doi.org/10.1162/jocn_a_00998
- 917 Panis, S., & Schmidt, T. (2022). When does “inhibition of return” occur in spatial cueing
918 tasks? Temporally disentangling multiple cue-triggered effects using response history
919 and conditional accuracy analyses. *Open Psychology*, 4(1), 84–114.
920 <https://doi.org/10.1515/psych-2022-0005>
- 921 Panis, S., Torfs, K., Gillebert, C. R., Wagemans, J., & Humphreys, G. W. (2017).
922 Neuropsychological evidence for the temporal dynamics of category-specific naming.
923 *Visual Cognition*, 25(1-3), 79–99. <https://doi.org/10.1080/13506285.2017.1330790>
- 924 Panis, S., & Wagemans, J. (2009). Time-course contingencies in perceptual organization
925 and identification of fragmented object outlines. *Journal of Experimental Psychology:*
926 *Human Perception and Performance*, 35(3), 661–687.
927 <https://doi.org/10.1037/a0013547>
- 928 Pedersen, T. L. (2024). *Patchwork: The composer of plots*. Retrieved from
929 <https://CRAN.R-project.org/package=patchwork>
- 930 Pinheiro, J. C., & Bates, D. M. (2000). *Mixed-effects models in s and s-PLUS*. New York:
931 Springer. <https://doi.org/10.1007/b98882>

- 932 R Core Team. (2024). *R: A language and environment for statistical computing*. Vienna,
933 Austria: R Foundation for Statistical Computing. Retrieved from
934 <https://www.R-project.org/>
- 935 Ripley, B., Venables, B., Bates, D. M., ca 1998), K. H. (partial. port, ca 1998), A. G.
936 (partial. port, & polr), D. F. (support. functions for. (2024). *MASS: Support Functions*
937 and *Datasets for Venables and Ripley's MASS*.
- 938 Singer, J. D., & Willett, J. B. (2003). *Applied Longitudinal Data Analysis: Modeling
939 Change and Event Occurrence*. Oxford, New York: Oxford University Press.
- 940 Smith, P. L., & Little, D. R. (2018). Small is beautiful: In defense of the small-N design.
941 *Psychonomic Bulletin & Review*, 25(6), 2083–2101.
942 <https://doi.org/10.3758/s13423-018-1451-8>
- 943 Steele, F., Goldstein, H., & Browne, W. (2004). A general multilevel multistate competing
944 risks model for event history data, with an application to a study of contraceptive use
945 dynamics. *Statistical Modelling*, 4(2), 145–159.
946 <https://doi.org/10.1191/1471082X04st069oa>
- 947 Teachman, J. D. (1983). Analyzing social processes: Life tables and proportional hazards
948 models. *Social Science Research*, 12(3), 263–301.
949 [https://doi.org/10.1016/0049-089X\(83\)90015-7](https://doi.org/10.1016/0049-089X(83)90015-7)
- 950 Townsend, J. T. (1990). Truth and consequences of ordinal differences in statistical
951 distributions: Toward a theory of hierarchical inference. *Psychological Bulletin*, 108(3),
952 551–567. <https://doi.org/10.1037/0033-2909.108.3.551>
- 953 Wickelgren, W. A. (1977). Speed-accuracy tradeoff and information processing dynamics.
954 *Acta Psychologica*, 41(1), 67–85. [https://doi.org/10.1016/0001-6918\(77\)90012-9](https://doi.org/10.1016/0001-6918(77)90012-9)
- 955 Wickham, H. (2016). *ggplot2: Elegant graphics for data analysis*. Springer-Verlag New
956 York. Retrieved from <https://ggplot2.tidyverse.org>
- 957 Wickham, H. (2023a). *Forcats: Tools for working with categorical variables (factors)*.
958 Retrieved from [https://forcats.tidyverse.org/](https://forcats.tidyverse.org)

- 959 Wickham, H. (2023b). *Stringr: Simple, consistent wrappers for common string operations.*
960 Retrieved from <https://stringr.tidyverse.org>
- 961 Wickham, H., Averick, M., Bryan, J., Chang, W., McGowan, L. D., François, R., ...
962 Yutani, H. (2019). Welcome to the tidyverse. *Journal of Open Source Software*, 4(43),
963 1686. <https://doi.org/10.21105/joss.01686>
- 964 Wickham, H., Çetinkaya-Rundel, M., & Grolemund, G. (2023). *R for data science: Import,
965 tidy, transform, visualize, and model data* (2nd edition). Beijing Boston Farnham
966 Sebastopol Tokyo: O'Reilly.
- 967 Wickham, H., François, R., Henry, L., Müller, K., & Vaughan, D. (2023). *Dplyr: A
968 grammar of data manipulation.* Retrieved from <https://dplyr.tidyverse.org>
- 969 Wickham, H., & Henry, L. (2023). *Purrr: Functional programming tools.* Retrieved from
970 <https://purrr.tidyverse.org/>
- 971 Wickham, H., Hester, J., & Bryan, J. (2024). *Readr: Read rectangular text data.* Retrieved
972 from <https://readr.tidyverse.org>
- 973 Wickham, H., Vaughan, D., & Girlich, M. (2024). *Tidyr: Tidy messy data.* Retrieved from
974 <https://tidyr.tidyverse.org>
- 975 Winter, B. (2019). *Statistics for Linguists: An Introduction Using R.* New York:
976 Routledge. <https://doi.org/10.4324/9781315165547>
- 977 Wolkersdorfer, M. P., Panis, S., & Schmidt, T. (2020). Temporal dynamics of sequential
978 motor activation in a dual-prime paradigm: Insights from conditional accuracy and
979 hazard functions. *Attention, Perception, & Psychophysics*, 82(5), 2581–2602.
980 <https://doi.org/10.3758/s13414-020-02010-5>

981

Supplementary material

982 **A. Definitions of discrete-time hazard, survivor, probability mass, and**
 983 **conditional accuracy functions**

984 The shape of a distribution of waiting times can be described in multiple ways (Luce,
 985 1991). After dividing time in discrete, contiguous time bins indexed by t , let RT be a
 986 discrete random variable denoting the rank of the time bin in which a particular person's
 987 response occurs in a particular experimental condition. Because waiting times can only
 988 increase, discrete-time EHA focuses on the discrete-time hazard function

$$989 \quad h(t) = P(RT = t | RT \geq t) \quad (1)$$

990 and the discrete-time survivor function

$$991 \quad S(t) = P(RT > t) = [1-h(t)].[1-h(t-1)].[1-h(t-2)] \dots [1-h(1)] \quad (2)$$

992 and not on the probability mass function

$$993 \quad P(t) = P(RT = t) = h(t).S(t-1) \quad (3)$$

994 nor the cumulative distribution function

$$995 \quad F(t) = P(RT \leq t) = 1-S(t) \quad (4)$$

996 The discrete-time hazard function of event occurrence gives you for each bin the
 997 probability that the event occurs (sometime) in that bin, given that the event has not
 998 occurred yet in previous bins. This conditionality in the definition of hazard is what makes
 999 the hazard function so diagnostic for studying event occurrence, as an event can physically
 1000 not occur when it has already occurred before. While the discrete-time hazard function
 1001 assesses the unique risk of event occurrence associated with each time bin, the
 1002 discrete-time survivor function cumulates the bin-by-bin risks of event *non*occurrence to
 1003 obtain the probability that the event occurs after bin t . The probability mass function
 1004 cumulates the risk of event occurrence in bin t with the risks of event nonoccurrence in

1005 bins 1 to $t-1$. From equation 3 we find that hazard in bin t is equal to $P(t)/S(t-1)$.

1006 For two-choice RT data, the discrete-time hazard function can be extended with the
 1007 discrete-time conditional accuracy function

$$1008 \quad ca(t) = P(\text{correct} \mid RT = t) \quad (5)$$

1009 which gives you for each bin the probability that a response is correct given that it is
 1010 emitted in time bin t (Allison, 2010; Kantowitz & Pachella, 2021; Wickelgren, 1977). This
 1011 latter function is also known as the micro-level speed-accuracy tradeoff (SAT) function.

1012 The survivor function provides a context for the hazard function, as $S(t-1) = P(RT >$
 1013 $t-1) = P(RT \geq t)$ tells you on how many percent of the trials the estimate $h(t) = P(RT =$
 1014 $t \mid RT \geq t)$ is based. The probability mass function provides a context for the conditional
 1015 accuracy function, as $P(t) = P(RT = t)$ tells you on how many percent of the trials the
 1016 estimate $ca(t) = P(\text{correct} \mid RT = t)$ is based.

1017 While psychological RT data is typically measured in small, continuous units (e.g.,
 1018 milliseconds), discrete-time EHA treats the RT data as interval-censored data, because it
 1019 only uses the information that the response occurred sometime in a particular bin of time
 1020 $(x,y]: x < RT \leq y$. If we want to use the exact event times, then we treat time as a
 1021 continuous variable, and let RT be a continuous random variable denoting a particular
 1022 person's response time in a particular experimental condition. Continuous-time EHA does
 1023 not focus on the cumulative distribution function $F(t) = P(RT \leq t)$ and its derivative, the
 1024 probability density function $f(t) = F(t)'$, but on the survivor function $S(t) = P(RT > t)$
 1025 and the hazard rate function $\lambda(t) = f(t)/S(t)$. The hazard rate function gives you the
 1026 instantaneous *rate* of event occurrence at time point t , given that the event has not
 1027 occurred yet.

1028 **B. Custom functions for descriptive discrete-time hazard analysis**

1029 We defined 12 custom functions that we list here.

- censor(df,timeout,bin_width) : divide the time segment $(0, \text{timeout}]$ in bins, identify any right-censored observations, and determine the discrete RT (time bin rank)
- ptb(df) : transform the person-trial data set to the person-trial-bin data set
- setup_lt(ptb) : set up a life table for each level of 1 independent variable
- setup_lt_2IV(ptb) : set up a life table for each combination of levels of 2 independent variables
- calc_ca(df) : estimate the conditional accuracies when there is 1 independent variable
- calc_ca_2IV(df) : estimate the conditional accuracies when there are 2 independent variables
- join_lt_ca(df1,df2) : add the $\text{ca}(t)$ estimates to the life tables (1 independent variable)
- join_lt_ca_2IV(df1, df2) : add the $\text{ca}(t)$ estimates to the life tables (2 independent variables)
- extract_median(df) : estimate quantiles $S(t)._{50}$ (1 independent variable)
- extract_median_2IV(df) : estimate quantiles $S(t)._{50}$ (2 independent variables)
- plot_eha(df, subj, haz_yaxis=1, first_bin_shown=1, aggregated_data=F, Nsubj=6) : create plots of the discrete-time functions (1 independent variable), and specify the upper limit of the y-axis in the hazard plot, with which bin to start plotting, whether the data is aggregated across participants, and across how many participants
- plot_eha_2IV(df, subj, haz_yaxis=1, first_bin_shown=1, aggregated_data=F, Nsubj=6) : create plots of the discrete-time functions (2 independent variables), and specify the upper limit of the y-axis in the hazard plot, with which bin to start plotting, whether the data is aggregated across participants, and across how many participants

When you want to analyse simple RT data from a detection experiment with one independent variable, the functions calc_ca() and join_lt_ca() should not be used, and the code to plot the conditional accuracy functions should be removed from the function

1057 plot_eha(). When you want to analyse simple RT data from a detection experiment with
1058 two independent variables, the functions calc_ca_2IV() and join_lt_ca_2IV() should not
1059 be used, and the code to plot the conditional accuracy functions should be removed from
1060 the function plot_eha_2IV().

1061 **C. Link functions**

1062 Popular link functions include the logit link and the complementary log-log link, as
1063 shown in Figure 15.

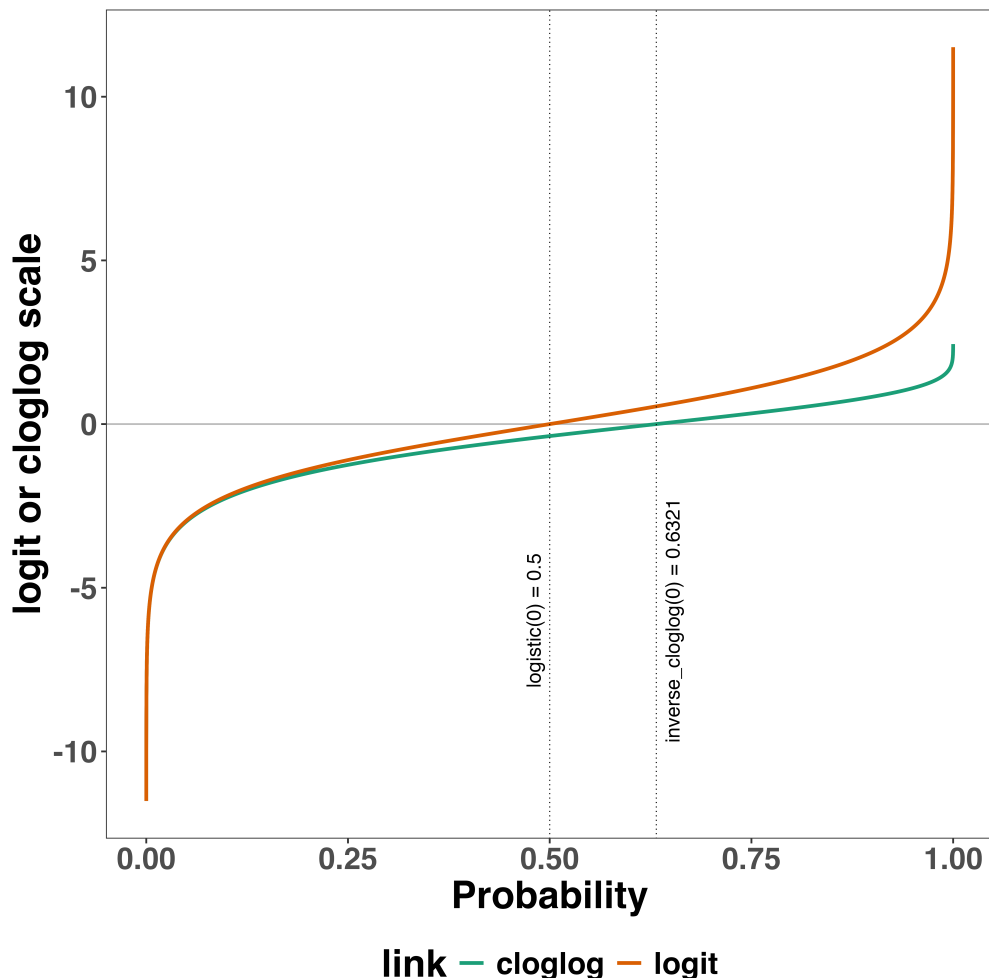


Figure 15. The logit and cloglog link functions.

¹⁰⁶⁴ **D. Regression equations**

¹⁰⁶⁵ An example (single-level) discrete-time hazard model with three predictors (TIME,
¹⁰⁶⁶ X₁, X₂), the cloglog link function, and a second-order polynomial specification for TIME
¹⁰⁶⁷ can be written as follows:

$$\begin{aligned} \text{cloglog}[h(t)] &= \ln(-\ln[1-h(t)]) = [\beta_0 \text{ONE} + \beta_1(\text{TIME}-9) + \beta_2(\text{TIME}-9)^2] + [\beta_3 X_1 + \beta_4 X_2 \\ &\quad + \beta_5 X_2(\text{TIME}-9)] \end{aligned} \quad (6)$$

¹⁰⁷⁰ The main predictor variable TIME is the time bin index t that is centered on value 9
¹⁰⁷¹ in this example. The first set of terms within brackets, the parameters β_0 to β_2 multiplied
¹⁰⁷² by their polynomial specifications of (centered) time, represents the shape of the baseline
¹⁰⁷³ cloglog-hazard function (i.e., when all predictors X_i take on a value of zero). The second
¹⁰⁷⁴ set of terms (the beta parameters β_3 to β_5) represents the vertical shift in the baseline
¹⁰⁷⁵ cloglog-hazard for a 1 unit increase in the respective predictor variable. Predictors can be
¹⁰⁷⁶ discrete, continuous, and time-varying or time-invariant. For example, the effect of a 1 unit
¹⁰⁷⁷ increase in X₁ is to vertically shift the whole baseline cloglog-hazard function by β_3
¹⁰⁷⁸ cloglog-hazard units. However, if the predictor interacts linearly with TIME (see X₂ in the
¹⁰⁷⁹ example), then the effect of a 1 unit increase in X₂ is to vertically shift the predicted
¹⁰⁸⁰ cloglog-hazard in bin 9 by β_4 cloglog-hazard units (when TIME-9 = 0), in bin 10 by $\beta_4 +$
¹⁰⁸¹ β_5 cloglog-hazard units (when TIME-9 = 1), and so forth. To interpret the effects of a
¹⁰⁸² predictor, its β parameter is exponentiated, resulting in a hazard ratio (due to the use of
¹⁰⁸³ the cloglog link). When using the logit link, exponentiating a β parameter results in an
¹⁰⁸⁴ odds ratio.

¹⁰⁸⁵ An example (single-level) discrete-time hazard model with a general specification for
¹⁰⁸⁶ TIME (separate intercepts for each of six bins, where D1 to D6 are binary variables
¹⁰⁸⁷ identifying each bin) and a single predictor (X₁) can be written as follows:

$$\text{cloglog}[h(t)] = [\beta_0 D1 + \beta_1 D2 + \beta_2 D3 + \beta_3 D4 + \beta_4 D5 + \beta_5 D6] + [\beta_6 X_1] \quad (7)$$

E. Prior distributions

To gain a sense of what prior *logit* values would approximate a uniform distribution on the probability scale, Kurz (2023a) simulated a large number of draws from the Uniform(0,1) distribution, converted those draws to the log-odds metric, and fitted a Student's t distribution. Row C in Figure 16 shows that using a t-distribution with 7.61 degrees of freedom and a scale parameter of 1.57 as a prior on the logit scale, approximates a uniform distribution on the probability scale. According to Kurz (2023a), such a prior might be a good prior for the intercept(s) in a logit-hazard model, while the N(0,1) prior in row D might be a good prior for the non-intercept parameters in a logit-hazard model, as it gently regularizes p towards .5 (i.e., a zero effect on the logit scale).

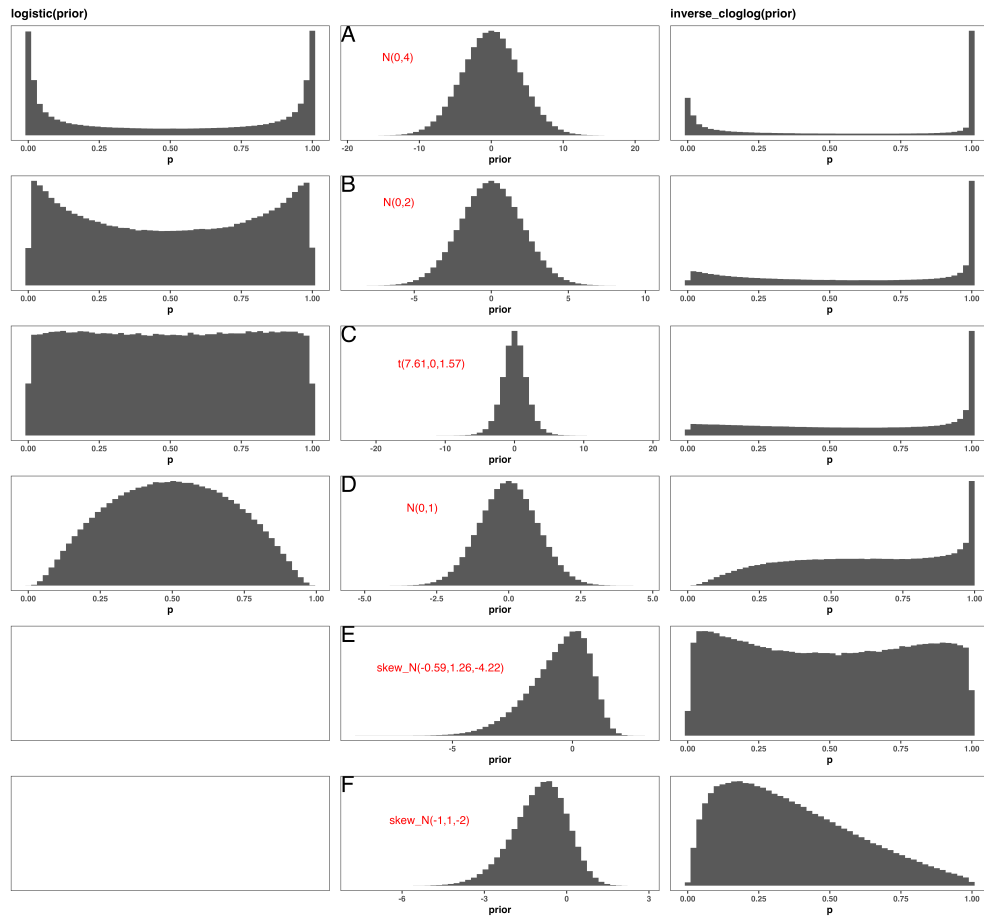


Figure 16. Prior distributions for the Intercept on the logit and/or cloglog scales (middle column), and their implications on the probability scale after applying the inverse-logit (or logistic) transformation (left column), and the inverse-cloglog transformation (right column).

1099 To gain a sense of what prior *cloglog* values would approximate a uniform distribution
 1100 on the hazard probability scale, we followed Kurz's approach and simulated a large number
 1101 of draws from the Uniform(0,1) distribution, converted them to the cloglog metric, and
 1102 fitted a skew-normal model (due to the asymmetry of the cloglog link function). Row E
 1103 shows that using a skew-normal distribution with a mean of -0.59, a standard deviation of
 1104 1.26, and a skewness of -4.22 as a prior on the cloglog scale, approximates a uniform
 1105 distribution on the probability scale. However, because hazard values below .5 are more
 1106 likely in RT studies, using a skew-normal distribution with a mean of -1, a standard

1107 deviation of 1, and a skewness of -2 as a prior on the cloglog scale (row F), might be a good
1108 weakly informative prior for the intercept(s) in a cloglog-hazard model.

1109 **F. Advantages of hazard analysis**

1110 Statisticians and mathematical psychologists recommend focusing on the hazard
1111 function when analyzing time-to-event data for various reasons. First, as discussed by
1112 Holden, Van Orden, and Turvey (2009), “probability density [and mass] functions can
1113 appear nearly identical, both statistically and to the naked eye, and yet are clearly different
1114 on the basis of their hazard functions (but not vice versa). Hazard functions are thus more
1115 diagnostic than density functions” (p. 331) when one is interested in studying the detailed
1116 shape of a RT distribution (see also Figure 1 in Panis, Schmidt, et al., 2020). Therefore,
1117 when the goal is to study how psychological effects change over time, hazard and
1118 conditional accuracy functions are the preferred ways to describe the RT + accuracy data.

1119 Second, because RT distributions may differ from one another in multiple ways,
1120 Townsend (1990) developed a dominance hierarchy of statistical differences between two
1121 arbitrary distributions A and B. For example, if $h_A(t) > h_B(t)$ for all t, then both hazard
1122 functions are said to show a complete ordering. Townsend (1990) concluded that stronger
1123 conclusions can be drawn from data when comparing the hazard functions using EHA. For
1124 example, when mean A < mean B, the hazard functions might show a complete ordering
1125 (i.e., for all t), a partial ordering (e.g., only for $t > 300$ ms, or only for $t < 500$ ms), or they
1126 may cross each other one or more times.

1127 Third, EHA does not discard right-censored observations when estimating hazard
1128 functions, that is, trials for which we do not observe a response during the data collection
1129 period in a trial so that we only know that the RT must be larger than some value (e.g.,
1130 the response deadline). This is important because although a few right-censored
1131 observations are inevitable in most RT tasks, a lot of right-censored observations are

expected in experiments on masking, the attentional blink, and so forth. In other words, by using EHA you can analyze RT data from experiments that typically do not measure response times. As a result, EHA can also deal with long RTs in experiments without a response deadline, which are typically treated as outliers and are discarded before calculating a mean. This orthodox procedure leads to underestimation of the true mean. By introducing a fixed censoring time for all trials at the end of the analysis time window, trials with long RTs are not discarded but contribute to the risk set of each bin.

Fourth, hazard modeling allows incorporating time-varying explanatory covariates such as heart rate, electroencephalogram (EEG) signal amplitude, gaze location, etc. (Allison, 2010). This is useful for linking physiological effects to behavioral effects when performing cognitive psychophysiology (Meyer et al., 1988).

Finally, as explained by Kelso, Dumas, and Tognoli (2013), it is crucial to first have a precise description of the macroscopic behavior of a system (here: $h(t)$ and possibly $ca(t)$ functions) in order to know what to derive on the microscopic level. EHA can thus solve the problem of model mimicry, i.e., the fact that different computational models can often predict the same mean RTs as observed in the empirical data, but not necessarily the detailed shapes of the empirical RT hazard distributions. Also, fitting parametric functions or computational models to data without studying the shape of the empirical discrete-time $h(t)$ and $ca(t)$ functions can miss important features in the data (Panis, Moran, et al., 2020; Panis & Schmidt, 2016).